
Joints in Random Forests

Alvaro H. C. Correia
Eindhoven University of Technology

Robert Peharz
Eindhoven University of Technology

Cassio P. de Campos
Eindhoven University of Technology

Abstract

Decision Trees (DTs) and Random Forests (RFs) are powerful discriminative learners and tools of central importance to the everyday machine learning practitioner and data scientist. Due to their discriminative nature, however, they lack principled methods to process inputs with missing features or to detect outliers, which requires pairing them with imputation techniques or a separate generative model. In this paper, we demonstrate that DTs and RFs can naturally be interpreted as generative models, by drawing a connection to Probabilistic Circuits, a prominent class of tractable probabilistic models. This reinterpretation equips them with a full joint distribution over the feature space and leads to Generative Decision Trees (GeDTs) and Generative Forests (GeFs), a family of novel hybrid generative-discriminative models. This family of models retains the overall characteristics of DTs and RFs while additionally being able to handle missing features by means of marginalisation. Under certain assumptions, frequently made for Bayes consistency results, we show that consistency in GeDTs and GeFs extend to any pattern of missing input features, if missing at random. Empirically, we show that our models often outperform common routines to treat missing data, such as K-nearest neighbour imputation, and moreover, that our models can naturally detect outliers by monitoring the marginal probability of input features.

1 Introduction

Decision Trees (DTs) and Random Forests (RFs) are probably the most widely used non-linear machine learning models of today. While Deep Neural Networks are in the lead for image, video, audio, and text data—likely due to their beneficial inductive bias for signal-like data—DTs and RFs are, by and large, the default predictive model for tabular, domain-agnostic datasets. Indeed, Kaggle’s 2019 report on the *State of Data Science and Machine Learning* [23] lists DTs and RFs as second most widely used techniques, right after linear and logistic regressions. Moreover, a study by Fernandez et al. [13] found that RFs performed best on 121 UCI datasets against 179 other classifiers. Thus, it is clear that DTs and RFs are of central importance for the current machine learning practitioner.

DTs and RFs are generally understood as *discriminative models*, that is, they are solely interpreted as predictive models, such as *classifiers* or *regression functions*, while attempts to additionally interpret them as *generative* models are scarce. In a nutshell, the difference between discriminative and generative models is that the former aim to capture the *conditional distribution* $P(Y | \mathbf{X})$, while the latter aim to capture the whole *joint distribution* $P(Y, \mathbf{X})$, where \mathbf{X} are the input features and Y is the variable to be predicted—discrete for classification and continuous for regression. In this paper, we focus on classification, but the extension to regression is straightforward.

Generative and discriminative models are rather complementary in their strengths and use cases. While discriminative models typically fare better in predictive performance, generative models allow to analyse and capture the structure present in the input space. They are also “all-round predictors”, that is, not restricted to a single prediction task but also capable of predicting any X given $Y \cup \mathbf{X} \setminus X$. Moreover, generative models have some crucial advantages on the prediction task $P(Y | \mathbf{X})$ a discriminative model has been trained on, as they naturally allow to *detect outliers* (by monitoring $P(\mathbf{X})$) and *treat missing features* (by marginalisation). A purely discriminative model does not have any “innate” mechanisms to deal with these problems, and needs to be supported with a generative model $P(\mathbf{X})$ (to detect outliers) or imputation techniques (to handle missing features).

Ideally, we would like the best of both worlds: having the good predictive performance of discriminative models *and* the advantages of generative models. In this paper, we show that this is achievable for DTs and RFs by relating them to *probabilistic circuits* (PCs) [54], a class of generative models based on computational graphs of *sum nodes* (mixtures), *product nodes* (factorisations), and *leaf nodes* (distribution functions). PCs subsume and represent a wide family of related models, such as *arithmetic circuits* [9], *AND/OR-graphs* [34], *sum-product networks* [41], *cutset networks* (C Nets) [47], and *probabilistic sentential decision diagrams* [26]. While many researchers are aware of the similarity between DTs and PCs—most notably, C Nets [47] can be seen as a type of generative DT—the connection to classical, discriminative DTs [43] and RFs [3] has not been studied so far.

We show that DTs and RFs can be naturally cast into the PC framework. For any given DT, we can construct a corresponding PC, denoted as *Generative Decision Tree* (GeDT), representing a full joint distribution $P(Y, \mathbf{X})$. This distribution gives rise to the predictor $P(Y | \mathbf{X}) = P(Y, \mathbf{X}) / \sum_y P(y, \mathbf{X})$, which is identical to the original DT, if we impose certain constraints on the conversion from DT to GeDT. Additionally, a GeDT also fits the joint distribution $P(\mathbf{X})$ to the training data, “upgrading” the DT to a full generative model. For a *completely observed sample* $\mathbf{X} = \mathbf{x}$, the original DT and its corresponding GeDT agree entirely (yield the exact same predictions), and moreover, have the *same computational complexity* (a discussion on time complexity is deferred to the appendix). By converting each DT in an RF into an GeDT, we obtain an ensemble of GeDTs, which we call *Generative Forest* (GeF). Clearly, if each GeDT in a GeF agrees with its original DT, then GeFs also agree with their corresponding RFs.

GeDTs and GeFs have a crucial advantage in the case of *missing features*, that is, assignments $\mathbf{X}_o = \mathbf{x}_o$ for some subset $\mathbf{X}_o \subset \mathbf{X}$, while $\mathbf{X}_{-o} = \mathbf{X} \setminus \mathbf{X}_o$ are *missing at random*. In a GeDT, we can marginalise the missing features and yield the predictor

$$P(Y | \mathbf{X}_o) = \frac{\int_{\mathbf{x}_{-o}} P(Y, \mathbf{X}_o, \mathbf{x}_{-o}) d\mathbf{x}_{-o}}{\sum_y \int_{\mathbf{x}_{-o}} P(y, \mathbf{X}_o, \mathbf{x}_{-o}) d\mathbf{x}_{-o}}. \quad (1)$$

For GeFs, we yield a corresponding ensembled predictor for missing features, by applying marginalisation to each GeDT. Using the true data generating distribution in Eq. (1) would deliver the *Bayes optimal predictor* for any subset \mathbf{X}_o of observed features. Thus, since GeDTs are trained to approximate the true distribution, using the predictor of Eq. (1) under missing data is well justified. We show that GeDTs are in fact *consistent*, i.e. they converge to the Bayes optimal classifier when the number of data points goes to infinity. Our proof requires similar assumptions as previous consistency results of DTs [1, 5, 18] but is substantially more general: while consistency in DTs is shown only for a classifier $P(Y | \mathbf{X})$ using fully observed samples, our consistency result holds for *all* $2^{|\mathbf{X}|}$ classifiers $P(Y | \mathbf{X}_o)$; one for each observation pattern $\mathbf{X}_o \subseteq \mathbf{X}$. While the high-dimensional integrals in Eq. (1) seem prohibitive, they are in fact *tractable*, since a remarkable feature of PCs is that computing any marginal has *the same complexity* as evaluating the full joint, namely linear in the *circuit size*.

This ability of our models is desirable, as there is no clear consensus on how to deal with missing features in DTs at test time: The most common strategy is to use *imputation*, e.g. *mean* or *k-nearest-neighbour (KNN) imputation*, and subsequently feeding the completed sample to the classifier. DTs also have two “built-in” methods to deal with missing features that do not require external models. These are the so-called *surrogate splits* [53] and an unnamed method proposed by Friedman in 1977 [15, 44]. Among these, KNN imputation seems to be the most widely used, and typically delivers good results on real-world data. However, we demonstrate it does not lead to a consistent predictor under missing data, even when assuming idealised settings. Moreover, in our experiments, we show that GeF classification under missing inputs often outperforms standard RFs with KNN imputation.

Our generative interpretation can be easily incorporated in existing DT learners and does not require drastic changes in the learning and application practice for DTs and RFs. Essentially, any DT algorithm can be used to learn GeDTs, requiring only minor bookkeeping and some extra generative learning steps. There are de facto no model restrictions concerning the additional generative learning steps, representing a generic scheme to augment DTs and RFs to generative models.

2 Notation and Background

In this paper we focus on classification tasks. To this end, let the set of explanatory variables (features) be $\mathbf{X} = \{X_1, X_2, \dots, X_m\}$, where continuous X_i assume values in some compact set $\mathcal{X}_i \subset \mathbb{R}$ and discrete X_i assume values in $\mathcal{X}_i = \{1, \dots, K_i\}$, where K_i is the number of states for X_i . Let the joint *feature space* of \mathbf{X} be denoted as \mathcal{X} . We denote joint states, i.e. elements from \mathcal{X} , as \mathbf{x} and let $\mathbf{x}[i]$ be the state in \mathbf{x} belonging to X_i . The class variable is denoted as Y , assuming values in $\mathcal{Y} = \{1, \dots, K\}$, where K is the number of classes. We assume that the pair (\mathbf{X}, Y) is drawn from a fixed joint distribution $\mathbb{P}^*(\mathbf{X}, Y)$ which has density $p^*(\mathbf{X}, Y)$. While the true distribution \mathbb{P}^* is unknown, we assume that we have a dataset $\mathcal{D}_n = \{(\mathbf{x}_1, y_1), \dots, (\mathbf{x}_n, y_n)\}$ of n i.i.d. samples from \mathbb{P}^* . When describing a directed graph \mathcal{G} , we refer to its set of nodes as V , reserving letters u and v for individual nodes. We denote the set of children and parents of a node v as $\text{ch}(v)$ and $\text{pa}(v)$, respectively. Nodes v without children are referred to as *leaves*, and nodes without parents are referred to as *roots*.

Decision Trees. A *decision tree* (DT) is based on a *rooted directed tree* \mathcal{G} , i.e. an acyclic directed graph with exactly one root v_r and whose other nodes have exactly one parent. Each node v in the DT is associated with a *cell* \mathcal{X}_v , which is a subset of the feature space \mathcal{X} . The cell of the root node v_r is whole \mathcal{X} . The *child cells* of node v form a partition of \mathcal{X}_v , i.e. $\bigcup_{u \in \text{ch}(v)} \mathcal{X}_u = \mathcal{X}_v$, $\mathcal{X}_u \cap \mathcal{X}_{u'} = \emptyset$, $\forall u, u' \in \text{ch}(v)$. These partitions are usually defined via *axis-aligned splits*, by associating a decision variable X_i to v , and partitioning the cell according to some rule on X_i 's values. Formally, we first project \mathcal{X}_v onto its i^{th} coordinate, yielding $\mathcal{X}_{i,v} := \{\mathbf{x}[i] \mid \mathbf{x} \in \mathcal{X}_v\}$, and construct a partition $\{\mathcal{X}_{i,u}\}_{u \in \text{ch}(v)}$ of $\mathcal{X}_{i,v}$. The child cells are then given by $\mathcal{X}_u = \{\mathbf{x} \mid \mathbf{x} \in \mathcal{X}_v \wedge \mathbf{x}[i] \in \mathcal{X}_{i,u}\}$. Common choices for this partition are *full splits* for discrete variables, i.e. choosing $\{\mathcal{X}_{i,u}\}_{u \in \text{ch}(v)} = \{\{x_i\}\}_{x_i \in \mathcal{X}_{i,v}}$ where children u and states x_i are in one-to-one correspondence, and *thresholding* for continuous variables, i.e. choosing $\{\mathcal{X}_{i,u}\}_{u \in \text{ch}(v)} = \{\{x_i < t\}, \{x_i \geq t\}\}$ for some threshold t . Note that the leaf cells of a DT represent a partition \mathcal{A} of the feature space \mathcal{X} . We denote the elements of \mathcal{A} as \mathcal{A} and define $\mathcal{A}_v = \mathcal{X}_v$ for each leaf v . A *DT classifier* is constructed by equipping each $\mathcal{A} \in \mathcal{A}$ with a classifier $f^{\mathcal{A}}: \mathcal{A} \mapsto \Delta^K$, where Δ^K is the set of probability distributions over K classes, i.e. $f^{\mathcal{A}}$ is a conditional distribution defined on \mathcal{A} . This distribution is typically stored as absolute class counts of the training samples contained in \mathcal{A} .

The overall DT classifier is given as $f(\mathbf{x}) = f^{\mathcal{A}(\mathbf{x})}(\mathbf{x})$ where $\mathcal{A}(\mathbf{x})$ is the leaf cell containing \mathbf{x} ; $\mathcal{A}(\mathbf{x})$ is found by parsing the DT top-down, following the partitions (decisions) consistent with \mathbf{x} . This formulation captures the vast majority of DT classifiers proposed in the literature, notably CART [5] and ID3 [43]. The probably most widely used variant of DTs—which we also assume in this paper—is to define $f^{\mathcal{A}}$ as a constant function, returning the class proportions in cell \mathcal{A} . The $\arg \max$ of $f^{\mathcal{A}}(\mathbf{x})$ is equivalent to majority voting among all training samples which fall into the same cell. When learning a DT, the number of available training samples per cell reduces quickly, which leads to overfitting and requires pruning techniques [5, 35, 43, 45].

Random Forests. *Random Forests* (RFs) are ensembles of DTs which effectively counteract overfitting. Each DT in a RF is learned in a randomised fashion, by drawing a random sub-selection of variables at each learning step, containing only a fraction p of all variables, where typical values are $p = 0.3$ or $p = \sqrt{m}$. The resulting DTs are not pruned, but made “deep” until each leaf cell contains either only samples of one class or less than T samples, where typical values are $T \in \{1, 5, 10\}$. This yields low bias, but high variance in the randomised DTs, which makes them good candidates for *bagging* (bootstrap aggregation) [20]. Thus, to further increase the variability among the trees, each of them is learned on a *bootstrapped* version of the training data [3].

Probabilistic Circuits. In this paper, we relate DTs to *Probabilistic Circuits* (PCs) [54], a family of density representations facilitating many exact and efficient inference routines. PCs are, like DTs, based on a rooted acyclic directed graph \mathcal{G} , albeit one with different semantics. PCs are computational graphs with three types of nodes, namely i) distribution nodes, ii) sum nodes and iii)

Input : Decision Tree \mathcal{G} and training data \mathcal{D}
Output : Probabilistic Circuit \mathcal{G}'
let \mathcal{G}' be a structural copy of \mathcal{G} and let v' be the node in \mathcal{G}' which corresponds to v of \mathcal{G}
for root node v of \mathcal{G} , set $\mathcal{D}_v = \mathcal{D}$
for v **in** $\text{topdownsort}(V)$ **do**
 if v **is** *internal* **then**
 get partition $\mathcal{X}_{i,u}$ of decision variable X_i associated with v
 for $u \in \text{ch}(v)$ **do**
 let $w_{v'u'} = \frac{\sum_{\mathbf{x} \in \mathcal{D}_v} \mathbb{1}(\mathbf{x}[i] \in \mathcal{X}_{i,u})}{|\mathcal{D}_v|}$
 set $\mathcal{D}_u = \{\mathbf{x} \in \mathcal{D}_v \mid \mathbf{x}[i] \in \mathcal{X}_{i,u}\}$
 end
 let v' be a sum node $\sum_{u' \in \text{ch}(v')} w_{v'u'} u'$
 else
 let v' be a density $p_{v'}(\mathbf{x}, y)$ with support \mathcal{A}_v , learned from \mathcal{D}_v
 end
end

Algorithm 1: Converting DT to PC (GeDT).

product nodes. Distribution nodes are the leaves of \mathcal{G} , while sum and product nodes are the internal nodes. Each distribution node (leaf) v computes a probability density¹ over some subset $\mathbf{X}' \subseteq \mathbf{X}$, i.e. a normalised function $p_v(\mathbf{x}') : \mathcal{X}' \mapsto \mathbb{R}^+$ from the state space of \mathbf{X}' to the non-negative real numbers. The set of variables \mathbf{X}' over which the leaf computes a distribution is called the *scope* of v , and denoted by $\text{sc}(v) := \mathbf{X}'$. Given the scopes of the leaves, the scope of any internal node v (sum or product) is recursively defined as $\text{sc}(v) = \cup_{u \in \text{ch}(v)} \text{sc}(u)$. Sum nodes compute convex combinations over their children, i.e. if v is a sum node, then v computes $v(\mathbf{x}) = \sum_{u \in \text{ch}(v)} w_{v,u} u(\mathbf{x})$, where $w_{v,u} \geq 0$ and $\sum_{u \in \text{ch}(v)} w_{v,u} = 1$. Product nodes compute the product over their children, i.e. if v is a product node, then $v(\mathbf{x}) = \prod_{u \in \text{ch}(v)} u(\mathbf{x})$. The density $p(\mathbf{X})$ represented by an PC is the function computed by its root node, and can be evaluated with a feed-forward pass.

The main feature of PCs is that they facilitate a wide range of *tractable* inference routines, which go hand in hand with certain structural properties, defined as follows [9, 54]: i) A sum node v is called *smooth* if its children have all the same scope: $\text{sc}(u) = \text{sc}(u')$, for any $u, u' \in \text{ch}(v)$. ii) A product node v is called *decomposable* if its children have non-overlapping scopes: $\text{sc}(u) \cap \text{sc}(u') = \emptyset$, for any $u, u' \in \text{ch}(v)$, $u \neq u'$. A PC is smooth (respectively decomposable) if all its sums (respectively products) are smooth (respectively decomposable). Smoothness and decomposability are sufficient to ensure *tractable marginalisation* in PCs. In particular, assume that we wish to evaluate the density over $\mathbf{X}_o \subset \mathbf{X}$ for evidence $\mathbf{X}_o = \mathbf{x}_o$, while marginalising $\mathbf{X}_{-o} = \mathbf{X} \setminus \mathbf{X}_o$. In PCs, this task reduces to performing marginalisation at the leaves [40], that is, for each leaf v one marginalises $\text{sc}(v) \cap \mathbf{X}_{-o}$, and evaluates it for the values corresponding to $\text{sc}(v) \cap \mathbf{X}_o$. The desired marginal $p_{\mathbf{X}_o}(\mathbf{x}_o)$ results from evaluating internal nodes as in computing the complete density. Furthermore, a PC is called *deterministic* [9, 54] if it holds that for each complete sample \mathbf{x} , each sum node has at most one non-zero child. Determinism and decomposability are sufficient conditions for *efficient maximisation*, which again, like density evaluation and marginalisation, reduces to a single feedforward-pass.

3 Generative Decision Trees

Given a learned DT and the dataset $\mathcal{D} = \{(\mathbf{x}_1, y_1), \dots, (\mathbf{x}_n, y_n)\}$ it has been learned on, we can obtain a corresponding generative model, by converting the DT into a PC. This conversion is given in Algorithm 1. In a nutshell, Algorithm 1 converts each decision node into a sum node and each leaf into a density with support restricted to the leaf's cell. The training samples can be figured to be routed from the root node to the leaves, following the decisions at each decision/sum node. The sum weights are given by the fraction of samples which are routed from the sum node to each of its children. The leaf densities are learned on the data which arrives at the respective leaves.

¹By an adequate choice of the underlying measure, this also subsumes probability mass functions.

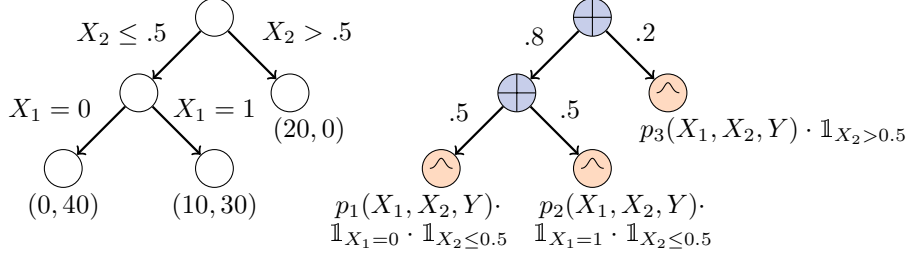


Figure 1: Illustration of a DT and its corresponding PC as obtained by Algorithm 1.

As an example, assuming \mathbf{X} and Y factorise at the leaves, Algorithm 1 applied to the DT on the left-hand side of Figure 1 gives the PC on the right-hand side and the following densities at the leaves:

$$\begin{aligned}
 p_1(X_1, X_2, Y) &= p_1(X_1, X_2)(0 \cdot \mathbb{1}(Y = 0) + 1 \cdot \mathbb{1}(Y = 1)), \\
 p_2(X_1, X_2, Y) &= p_2(X_1, X_2)(0.25 \cdot \mathbb{1}(Y = 0) + 0.75 \cdot \mathbb{1}(Y = 1)), \\
 p_3(X_1, X_2, Y) &= p_3(X_1, X_2)(1 \cdot \mathbb{1}(Y = 0) + 0 \cdot \mathbb{1}(Y = 1)),
 \end{aligned}$$

Note that X_1 is deterministic (all mass absorbed in one state) in p_1 and p_2 , since X_1 has been fixed by the tree construction, while p_3 is a “proper” distribution over X_1 and X_2 . Densities $p_i(X_1, X_2)$ do not appear in the DT representation and illustrate the extension brought in by the PC formalism.

We denote the output of Algorithm 1 as *Generative Decision Tree* (GeDT). Note that GeDTs are proper PCs over (\mathbf{X}, Y) , albeit rather simple ones: they are tree-shaped and contain only sum nodes. They are clearly smooth, since each leaf density has the full scope (\mathbf{X}, Y) , and they are trivially decomposable, as they do not contain products. Thus, both the full density or any sub-marginal can be evaluated by simply evaluating the GeDT bottom up, where for marginalisation tasks we first need to perform marginalisation at the leaves. Furthermore, it is easy to show that any GeDT is *deterministic* (see appendix). As shown in [38, 47], the sum-weights set by Algorithm 1 are in fact the *maximum likelihood* weights for deterministic PCs.

In Algorithm 1, we learn a density $p_v(\mathbf{x}, y)$ for each leaf v , where we have not yet specified the model or learning algorithm. Thus, we denote $\text{GeDT}(M)$ as a GeDT whose leaf densities are learned by “method M ”, where M might be graphical models, again PCs, or even neural-based density estimators [25, 49]. In order to ensure tractable marginalisation of the overall GeDT, however, we use either *fully factorised* leaves or PCs learned with *LearnSPN* [17]—in both cases marginalisation at the leaves is efficient, and hence in the whole GeDT. Regardless of the model M , we generally learn the leaves using the maximum likelihood principle, or some proxy of it. Thus, since the sum-weights are already set to the (global) maximum likelihood solution by Algorithm 1, the overall GeDT is fitted to the training data. A basic design choice is how to model the dependency between \mathbf{X} and Y at the leaves: We might assume independence between them, i.e. assume $p(\mathbf{x}, y) = p(\mathbf{x})p(y)$ (*class-factorised* leaves);² or simply pass the data over both \mathbf{X} and Y to a learning algorithm and let it determine the dependency structure itself (*full* leaves).

The main semantic difference between DTs and GeDTs is that a DT represents a classifier, i.e. a conditional distribution $f(\mathbf{x})$, while the corresponding GeDT represents a full joint distribution $p(\mathbf{X}, Y)$. The latter naturally lends itself towards classification by deriving the conditional distribution $p(Y | \mathbf{x}) \propto p(\mathbf{x}, Y)$. How are the original DT classifier $f(\mathbf{x})$ and the GeDT classifier $p(Y | \mathbf{x})$ related? In theory, $p(Y | \mathbf{x})$ might differ substantially from $f(\mathbf{x})$, since every feature might influence classification in a GeDT, even if it never appears in any decision node of the DT. In the case of class-factorised leaves, however, we obtain “backwards compatibility”.

Theorem 1. *Let f be a DT classifier and $p(Y | \mathbf{x})$ be a corresponding GeDT classifier, where each leaf in GeDT is class-factorised, i.e. of the form $p(Y)p(\mathbf{X})$, and where $p(Y)$ has been estimated in maximum-likelihood sense. Then $f(\mathbf{x}) = p(Y | \mathbf{x})$, provided that $p(\mathbf{x}) > 0$.*

²Note that such independence is only a context-specific one, conditional on the state of variables associated with sum nodes [39, 41]. This assumption does not represent global independence between \mathbf{X} and Y .

For space reasons, proofs and complexity results are deferred to the appendix. Theorem 3 shows that DTs and GeDTs yield exactly the same classifier for class-factorised leaves and complete data. DTs achieve their most impressive performance when used as an ensemble in RFs. It is straight-forward to convert each DT in an RF using Algorithm 1, yielding an ensemble of GeDTs. We call such an ensemble a *Generative Forest* (GeF). This result extends to ensembles, as clearly when all GeDTs in a GeF use class-factorised leaves, then according to Theorem 3, GeFs yield exactly the same prediction function as their corresponding RFs. This means that the everyday practitioner can safely replace RFs with class-factorised GeFs, gaining the ability to classify under *missing input data*.

4 Handling Missing Values

The probably most frequent strategy to deal with missing inputs in DTs and RFs is to use some *single imputation* technique, i.e. to first predict any missing input values based on the observed ones, and then use the imputed sample as input to the classifier. A particular prominent method is *K-nearest neighbour* (KNN) imputation, which typically works well in practice. This strategy, however, is not Bayes consistent and can in principle be arbitrarily bad. This can be shown with a simple example: Assume two multivariate Gaussian features X_1 and X_2 with $\text{var}(X_1) \geq \tau$, $\text{var}(X_2) \geq \tau$ for some $\tau > 0$, i.e. the variances of X_1 and X_2 are bounded from below. Let the conditional class distribution be $p(y | x_1, x_2) = \mathbb{1}(|x_2 - \mathbb{E}[X_2 | x_1]| > \epsilon)$, i.e. Y detects whether X_2 deviates more than ϵ from its mean, conditional on X_1 . Assume that X_2 is missing and use KNN to impute it, based on $X_1 = x_1$. KNN is known to be a consistent regressor, given that the number of neighbours goes to infinity, but vanishes in comparison to n [10]. Thus, the imputation for X_2 based on $X_1 = x_1$ converges to $\mathbb{E}[X_2 | x_1]$ which yields a constant prediction of $Y = 1$. Thus, by making ϵ arbitrarily small, we can push the classification error arbitrarily close to 1, while the true error goes to 0.

Assuming that inputs are missing at random [29] and that we have only inputs \mathbf{x}_o for some subset $\mathbf{X}_o \subset \mathbf{X}$, a GeDT naturally yields a classifier $p(y | \mathbf{X}_o)$, by marginalising missing features as in Eq. (1). Recall that marginalisation in PCs, and thus in GeDTs, can be performed with a single feed-forward pass, given that the GeDT’s leaves permit efficient marginalisation. In our experiments, we use either fully factorised leaves or PC leaves learned by LearnSPN [17], a prominent PC learner, such that we can efficiently and exactly evaluate $p(Y | \mathbf{X}_o)$ with one network pass. Thus, a GeDT represents in fact $2^{|\mathbf{X}|}$ classifiers, one for each missingness pattern. Since the true data distribution yields Bayes optimal classifiers for each \mathbf{X}_o , and since the parameters of GeDTs are learned in maximum likelihood sense, using the GeDT predictor $p(y | \mathbf{X}_o)$ for missing data is natural. For a simplified variant of GeDTs, we can show that they converge to the true distribution and are therefore Bayes consistent classifiers for each \mathbf{X}_o . Theorem 4 assumes w.l.o.g. that all \mathbf{X} are continuous.

Theorem 2. *Let \mathbb{P}^* be an unknown data generating distribution with density $p^*(\mathbf{X}, Y)$, and let \mathcal{D}_n be a dataset drawn i.i.d. from \mathbb{P}^* . Let \mathcal{G} be a DT learned with a DT learning algorithm, using axis-aligned splits. Let \mathcal{A}^n be the (rectangular) leaf cells produced by the learning algorithm. Assume it holds that i) $\lim_{n \rightarrow \infty} |\mathcal{A}^n|^{\log(n)/n} \rightarrow 0$ and ii) $\mathbb{P}^*(\{\mathbf{x} | \text{diam}(\mathcal{A}_x^n) > \gamma\}) \rightarrow 0$ almost surely for all $\gamma > 0$, where $\text{diam}(\mathcal{A})$ is the diameter of cell \mathcal{A} . Let \mathcal{G}' be the GeDT corresponding to \mathcal{G} , obtained via Algorithm 1, where for each leaf v , p_v is of the form $p_v(Y)p_v(\mathbf{X})$, with $p_v(\mathbf{X})$ uniform on \mathcal{A}_v and $p_v(Y)$ the maximum likelihood Categorical (fractions of class values of samples in \mathcal{A}_v). Then the GeDT distribution is l_1 -consistent, i.e. $\sum_y \int |p(\mathbf{x}, y) - p^*(\mathbf{x}, y)| d\mathbf{x} \rightarrow 0$, almost surely.*

Note that the assumptions in Theorem 4 are in line with consistency results for DTs, see for example [5, 10, 32], which all require, in some sense, that the number of cells vanishes in comparison to the number of samples and that the cell sizes shrink to zero. Theorem 4 naturally leads to the Bayes-consistency of GeDTs and GeFs under missing inputs.

Corollary 1. *Under assumptions of Theorem 4, any GeDT predictor $p(Y | \mathbf{X}_o)$, for $\mathbf{X}_o \subseteq \mathbf{X}$ is Bayes consistent.*

Corollary 2. *Assume a GeF whose GeDTs are learned under assumptions of Theorem 4. Then the GeF of GeDT predictors $p(Y | \mathbf{X}_o)$, for any $\mathbf{X}_o \subseteq \mathbf{X}$, is Bayes consistent.*

5 Related Work

Many variations of DTs and RFs have been proposed in the last decades, and in particular methods which aim to extend DT leaves with “non-trivial” models. Since the central idea in this paper is

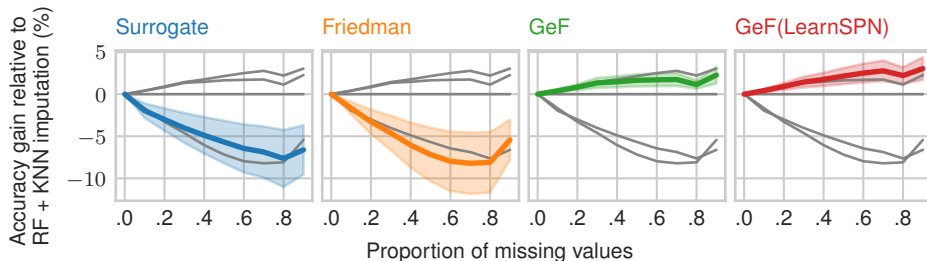


Figure 2: Average (across 21 datasets) accuracy gain relative to RFs (100 trees) plus KNN imputation against percent of missing values. Confidence intervals (95%) are also computed across the datasets.

to extend DTs to full joint models by augmenting their leaves with densities, we review the most similar works in this area. Notable examples are DTs with linear and logistic regressors [46, 14, 28], kernel density estimators (KDEs) [52, 30], linear discriminant models [16, 24], KNN classifiers [6, 30], and Naive-Bayes classifiers (NBCs) [27]. All these previous works focus primarily on improving the classification accuracy or smoothing probability estimates, but do not model the full joint distribution, like in this work. Even extensions by Smyth et al. [52] and Kohavi [27], which include generative models (KDEs and NBCs, respectively) do not exploit their generative properties. To the best of our knowledge, GeFs are the first DT framework that effectively model and leverage the full joint distribution in a classification context. That is of practical significance as none of these earlier extensions of DTs offer a principled way to treat missing values or detect outliers.

On the other side of the spectrum, DTs have also been extended to density estimators [19, 48, 47, 57]. Among these, Density Estimation Trees (DETs) [48], Cutset Networks (CNETs) [47], and randomised ensembles thereof [11], are probably the closest to our work. These models are trained with a greedy tree-learning algorithm but minimise a modified loss function that matches their generative nature—joint entropy across all variables in CNETs, mean integrated squared error in DETs. Notably, CNETs, like GeFs, are probabilistic circuits, and hence also allow for tractable inference and marginalisation. They, however, have not been applied in a discriminative setting and are not backwards compatible with DTs and RFs. Moreover, GeDTs (and GeFs) can be seen as a family of models depending on the estimation at the leaves, making a clear parallel with what DTs (and RFs) offer.

6 Experiments

We run a series of classification tasks with incomplete data to compare our models against surrogate splits [5, 53], Friedman’s method [15, 44], mean and KNN ($k = 7$) imputations [4, 50]. In particular, we experiment with fully-factorised (vanilla GeF) and *full* leaves learned with LearnSPN [17]. We use a transformation of GeFs into a clever PC that prunes unnecessary sub-trees [7], speeding up computations and achieving time complexity comparable to the original DTs and RFs (see appendix). In all experiments, GeF, GeF(LearnSPN) and the RF share the exact same structure (partition over the feature space) and are composed of 100 trees; including more trees has been shown to yield only marginal gains in most cases [42]. For the GeF(LearnSPN) models, we run LearnSPN only for leaves with more than 30 samples, defaulting to a fully factorised model in smaller leaves.

We compare accuracy of the methods in a selection of datasets from the OpenML-CC18 benchmark³ [55] and the wine-quality dataset [36]. Table 1 presents results for 30% of missing values at test time (different percentages are shown in the appendix). We report 95% confidence intervals across 10 repetitions of 5-fold cross-validation for small datasets ($n < 10000$) or a single 10-fold cross validation otherwise. GeF models outperform other methods in almost all datasets, validating that the joint distributions at the leaves provide enough information for computing the marginalisation in Eq. (1). We also note that increasing the expressive power of the models at the leaves seems worthwhile, as GeF(LSPN) outperforms the vanilla GeF in about half of the datasets, especially for

³<https://www.openml.org/s/99/data>

Table 1: Accuracy at 30% percent of missing values at test time with 95% confidence intervals. The best performing model is underlined, whereas all models within its confidence interval appear in bold.

Dataset	n	m_0	m_1	$ \mathcal{Y} $	Surrogate	Friedman	Mean*	KNN	GeF	GeF(LSPN)
dresses	500	12	0	2	45.84 ± .90	56.84 ± .50	<u>57.84</u> ± 1.23	56.08 ± .89	57.46 ± .86	57.44 ± .87
breast	569	0	30	2	94.36 ± .39	94.09 ± .39	93.64 ± .45	94.94 ± .47	95.24 ± .43	95.54 ± .47
diabetes	768	0	8	2	72.5 ± .43	73.2 ± .84	71.9 ± .64	72.32 ± .72	73.63 ± .65	73.59 ± .56
vehicle	846	0	18	4	71.48 ± .76	68.22 ± .92	61.95 ± 1.29	71.9 ± .63	72.99 ± .70	73.48 ± .64
vowel	990	2	10	11	76.42 ± 1.02	68.7 ± 1.10	63.93 ± .80	85.39 ± .85	89.3 ± .96	89.69 ± .99
german	1000	13	7	2	72.37 ± .41	73.18 ± .60	73.09 ± .76	73.02 ± .60	74.35 ± .55	74.39 ± .51
mice	1080	0	77	8	92.5 ± .40	86.66 ± .63	75.12 ± 1.04	96.56 ± .35	97.63 ± .26	98.79 ± .16
authent.	1372	0	4	2	86.84 ± .54	88.19 ± .47	84.53 ± .48	92.14 ± .31	90.33 ± .40	90.26 ± .27
cmc	1473	8	1	3	47.58 ± 1.34	49.46 ± .46	47.4 ± .80	48.04 ± .73	49.65 ± .75	49.59 ± .66
segment	2310	2	15	7	92.39 ± .14	82.74 ± .34	76.17 ± .69	94.13 ± .18	92.18 ± .18	92.73 ± .20
dna	3186	180	0	3	89.4 ± .31	81.29 ± .56	79.04 ± .43	87.25 ± .36	90.75 ± .40	87.89 ± .42
splice	3190	60	0	3	85.31 ± .43	83.59 ± .36	82.92 ± .44	87.94 ± .38	91.55 ± .25	87.49 ± .34
krvskp	3196	36	0	2	73.98 ± .79	82.12 ± .54	83.69 ± .35	86.7 ± .30	88.06 ± .17	88.75 ± .15
robot	5456	0	24	4	91.28 ± .29	85.32 ± .31	89.13 ± .33	92.41 ± .28	92.0 ± .31	93.85 ± .23
texture	5500	0	40	11	95.62 ± .62	84.89 ± 1.01	80.8 ± .75	97.25 ± .51	95.65 ± .47	97.0 ± .50
wine	6497	0	11	2	84.0 ± .10	82.09 ± .07	82.73 ± .10	85.77 ± .14	85.52 ± .15	86.03 ± .14
gesture	9873	0	32	5	57.77 ± 1.34	52.83 ± 1.16	54.61 ± 1.27	61.48 ± 1.52	59.25 ± 1.11	60.05 ± 1.13
phishing	11055	30	0	2	80.1 ± .82	88.69 ± .63	87.72 ± .53	91.74 ± .44	93.07 ± .53	93.5 ± .42
bank	41188	11	9	2	90.53 ± .24	90.31 ± .17	89.86 ± .16	90.59 ± .24	90.67 ± .16	90.59 ± .18
jungle	44819	6	0	3	63.65 ± .52	71.9 ± .27	67.12 ± .83	66.35 ± .48	72.5 ± .31	72.36 ± .27
electricity	45312	1	7	2	78.68 ± .22	77.08 ± .39	74.15 ± .62	80.17 ± .18	81.79 ± .31	82.43 ± .25

larger number of samples. Similar conclusions are supported by Figure 2, where we plot the average gain in accuracy relative to RF + KNN imputation at different proportions of missing values. While earlier built-in methods, Friedman’s and surrogate splits, perform poorly (justifying the popularity of imputation techniques for RFs), GeFs are about 5% more accurate than KNN imputation.

Another advantage of generative models is the ability of using the likelihood over the explanatory variables to detect outliers. GeFs are still an ensemble of generative GeDTs and thus do not encode a single full joint distribution. However, we can extend GeFs to model a single joint by considering a uniform mixture of GeDTs (using a sum node), instead of ensembling conditional distributions of each GeDT. In this case, the model represents the joint $p(\mathbf{X}, Y) = n_t^{-1} \sum_{j=1}^{n_t} p_j(\mathbf{X}, Y)$, where each p_j comes from a GeDT. This model is named GeF⁺ and achieves similar but slightly inferior performance than GeFs in classification with missing data (still clearly superior to KNN imputation). This does not come as a surprise: the benefits of a full generative models often comes at the cost of a (small) drop in classification accuracy (results in the appendix).

We use GeF⁺ on the the wine quality dataset [8] (where the class is a scale of quality of wine) with a variant of transfer testing [2]. We learn two different classifiers, each with only one type of wine (red or white), and compute the log-probabilities of unseen data (70/30 train test split) for the two wine types. As we see in the histograms of Figure 3, the marginal distribution over the joints does provide a strong signal to identify out-of-domain instances. Against a Gaussian Kernel Density Estimator (KDE), GeF⁺s achieve similar results even though their structure has been fit in a discriminative way.

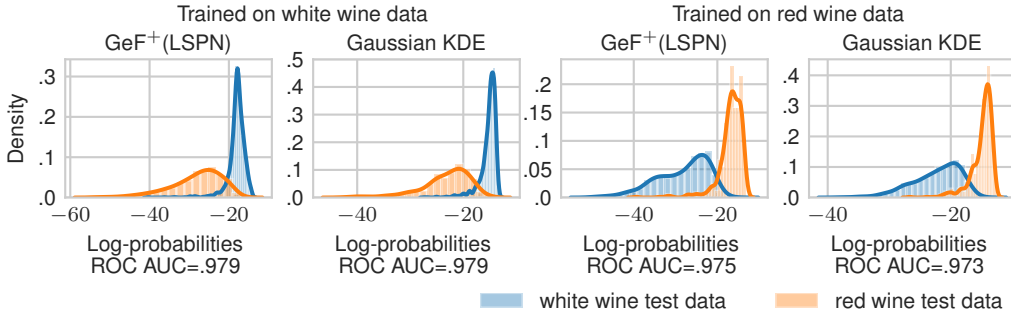


Figure 3: Log-probability normalised histograms of samples from two different wine datasets.

7 Conclusion

By establishing a connection between Decision Trees (DTs) and Probabilistic Circuits (PCs), we have upgraded DTs to a full joint model over both inputs and outputs, yielding their generative counterparts, called GeDTs. The fact that GeDTs, and their ensemble version GeFs, are “backwards compatible” to DTs and RFs, while offering benefits like consistent classification under missing inputs and outlier detection, makes it easy to adopt them in everyday practice. Missing data and outliers, however, are just the beginning. We believe that many of the current challenges in machine learning, like explainability, interpretability, and (adversarial) robustness, are but symptoms of an overemphasis of purely discriminative methods in the past decades, and that hybrid generative approaches—like the one in this paper—will contribute significantly towards mastering these current challenges.

References

- [1] G. Biau, L. Devroye, and G. Lugosi. Consistency of Random Forests and Other Averaging Classifiers. *Journal of Machine Learning Research*, 9:2015–2033, 2008.
- [2] J. Bradshaw, A. G. d. G. Matthews, and Z. Ghahramani. Adversarial examples, uncertainty, and transfer testing robustness in gaussian process hybrid deep networks. *arXiv preprint arXiv:1707.02476*, 2017.
- [3] L. Breiman. Random forests. *Machine Learning*, 45(1):5–32, 2001.
- [4] L. Breiman. Manual - Setting up, Using and Understanding Random Forests V4.0. Technical report, 2003.
- [5] L. Breiman, J. Friedman, C. J. Stone, and R. A. Olshen. *Classification and regression trees*. CRC press, 1984.
- [6] S. E. Buttrey and C. Karo. Using k-nearest-neighbor classification in the leaves of a tree. *Computational Statistics & Data Analysis*, 40(1):27–37, 2002.
- [7] A. Correia and C. de Campos. Towards scalable and robust sum-product networks. In *Scalable Uncertainty Management - 13th International Conference, SUM 2019, Proceedings*, Lecture Notes in Computer Science, pages 409–422, Germany, 2019. Springer.
- [8] P. Cortez, A. Cerdeira, F. Almeida, T. Matos, and J. Reis. Modeling wine preferences by data mining from physicochemical properties. *Decision Support Systems*, 47(4):547–553, nov 2009.
- [9] A. Darwiche. A differential approach to inference in Bayesian networks. *Journal of the ACM*, 50(3):280–305, 2003.
- [10] L. Devroye, L. Györfi, and G. Lugosi. *A Probabilistic Theory of Pattern Recognition*. Springer-Verlag, New York, 1996.
- [11] N. Di Mauro, A. Vergari, T. M. Basile, and F. Esposito. Fast and accurate density estimation with extremely randomized cutset networks. In *Joint European conference on machine learning and knowledge discovery in databases*, pages 203–219, 2017.
- [12] D. Dua and C. Graff. UCI machine learning repository, 2017.
- [13] M. Fernández-Delgado, E. Cernadas, S. Barro, and D. Amorim. Do we need hundreds of classifiers to solve real world classification problems? *The journal of machine learning research*, 15(1):3133–3181, 2014.
- [14] E. Frank, Y. Wang, S. Inglis, G. Holmes, and I. H. Witten. Using model trees for classification. *Machine learning*, 32(1):63–76, 1998.
- [15] J. H. Friedman. A recursive partitioning decision rule for nonparametric classification. *IEEE Transactions on Computers*, (4):404–408, 1977.
- [16] J. Gama, P. Medas, G. Castillo, and P. Rodrigues. Learning with drift detection. In *Brazilian symposium on artificial intelligence*, pages 286–295. Springer, 2004.
- [17] R. Gens and P. Domingos. Learning the Structure of Sum-Product Networks. In *Proceedings of the 30th International Conference on Machine Learning*, volume 28, pages 229–264, 2013.

- [18] L. Gordon and R. A. Olshen. Asymptotically efficient solutions to the classification problem. *The Annals of Statistics*, pages 515–533, 1978.
- [19] A. G. Gray and A. W. Moore. Nonparametric density estimation: Toward computational tractability. In *Proceedings of the 2003 SIAM International Conference on Data Mining*, pages 203–211. SIAM, 2003.
- [20] T. Hastie, R. Tibshirani, and J. Friedman. *The elements of statistical learning: data mining, inference, and prediction*. Springer Science & Business Media, 2009.
- [21] C. Higuera, K. J. Gardiner, and K. J. Cios. Self-organizing feature maps identify proteins critical to learning in a mouse model of down syndrome. *PloS one*, 10(6), 2015.
- [22] Z. Huang. Clustering large data sets with mixed numeric and categorical values," proceedings of 1st pacific-asia conference on knowledge discovery and data mining. 1997.
- [23] Kaggle. Kaggle’s State of Data Science and Machine Learning 2019. Technical report, 2019.
- [24] H. Kim and W.-Y. Loh. Classification trees with bivariate linear discriminant node models. *Journal of Computational and Graphical Statistics*, 12(3):512–530, 2003.
- [25] D. P. Kingma and M. Welling. Auto-encoding variational Bayes. In *ICLR*, 2014. arXiv:1312.6114.
- [26] D. Kisa, G. V. den Broeck, A. Choi, and A. Darwiche. Probabilistic Sentential Decision Diagrams. In *KR*, 2014.
- [27] R. Kohavi. Scaling Up the Accuracy of Naive-Bayes Classifiers: a Decision-Tree Hybrid. In *Knowledge Discovery and Data Mining (KDD)*, pages 202–217, 1996.
- [28] N. Landwehr, M. Hall, and E. Frank. Logistic model trees. *Machine learning*, 59(1-2):161–205, 2005.
- [29] R. J. Little and D. B. Rubin. *Statistical analysis with missing data*, volume 793. John Wiley & Sons, 2019.
- [30] W.-Y. Loh. Improving the precision of classification trees. *The Annals of Applied Statistics*, pages 1710–1737, 2009.
- [31] G. Louppe. *Understanding Random Forests: From Theory to Practice*. PhD thesis, University of Liege, 2014.
- [32] G. Lugosi, A. Nobel, et al. Consistency of data-driven histogram methods for density estimation and classification. *The Annals of Statistics*, 24(2):687–706, 1996.
- [33] R. C. Madeo, C. A. Lima, and S. M. Peres. Gesture unit segmentation using support vector machines: segmenting gestures from rest positions. In *Proceedings of the 28th Annual ACM Symposium on Applied Computing*, pages 46–52, 2013.
- [34] R. Marinescu and R. Dechter. And/or branch-and-bound for graphical models. In *IJCAI*, pages 224–229, 2005.
- [35] J. Mingers. Expert systems—rule induction with statistical data. *Journal of the operational research society*, 38(1):39–47, 1987.
- [36] S. Moro, R. Laureano, and P. Cortez. Using data mining for bank direct marketing: An application of the crisp-dm methodology. In *Proceedings of European Simulation and Modelling Conference-ESM’2011*, pages 117–121. EUROSIS-ETI, 2011.
- [37] F. Pedregosa, G. Varoquaux, A. Gramfort, V. Michel, B. Thirion, O. Grisel, M. Blondel, P. Prettenhofer, R. Weiss, V. Dubourg, J. Vanderplas, A. Passos, D. Cournapeau, M. Brucher, M. Perrot, and E. Duchesnay. Scikit-learn: Machine learning in Python. *Journal of Machine Learning Research*, 12:2825–2830, 2011.
- [38] R. Peharz, R. Gens, and P. Domingos. Learning selective sum-product networks. *Proceedings of the 31st International Conference on Machine Learning*, 32, 2014.
- [39] R. Peharz, R. Gens, F. Pernkopf, and P. Domingos. On the latent variable interpretation in sum-product networks. *IEEE transactions on pattern analysis and machine intelligence*, 39(10):2030–2044, 2016.
- [40] R. Peharz, S. Tschiatschek, F. Pernkopf, and P. Domingos. On theoretical properties of sum-product networks. In *Artificial Intelligence and Statistics*, pages 744–752, 2015.

- [41] H. Poon and P. Domingos. Sum-product networks: A new deep architecture. In *Proceedings of UAI*, pages 337–346, 2011.
- [42] P. Probst and A. L. Boulesteix. To tune or not to tune the number of trees in random forest. *Journal of Machine Learning Research*, 18:1–8, 2018.
- [43] J. R. Quinlan. Induction of decision trees. *Machine Learning*, 1(1):81–106, 1986.
- [44] J. R. Quinlan. Decision trees as probabilistic classifiers. In *Proceedings of the Fourth International Workshop on Machine Learning*, pages 31–37. Elsevier, 1987.
- [45] J. R. Quinlan. Simplifying decision trees. *International journal of man-machine studies*, 27(3):221–234, 1987.
- [46] J. R. Quinlan et al. Learning with continuous classes. In *5th Australian joint conference on artificial intelligence*, volume 92, pages 343–348. World Scientific, 1992.
- [47] T. Rahman, P. Kothalkar, and V. Gogate. Cutset networks: A simple, tractable, and scalable approach for improving the accuracy of chow-liu trees. In *Joint European conference on machine learning and knowledge discovery in databases*, pages 630–645, 2014.
- [48] P. Ram and A. G. Gray. Density estimation trees. *Proceedings of the ACM SIGKDD International Conference on Knowledge Discovery and Data Mining*, pages 627–635, 2011.
- [49] D. J. Rezende and S. Mohamed. Variational inference with normalizing flows. In *Proceedings of ICML*, pages 1530–1538, 2015.
- [50] M. Saar-Tsechansky and F. Provost. Handling missing values when applying classification models. *Journal of Machine Learning Research*, 8:1625–1657, 2007.
- [51] J. P. Siebert. Vehicle recognition using rule based methods. 1987.
- [52] P. Smyth, A. Gray, and U. M. Fayyad. Retrofitting Decision Tree Classifiers Using Kernel Density Estimation. *Machine Learning Proceedings*, 36:506–514, 1995.
- [53] T. M. Therneau, E. J. Atkinson, et al. An introduction to recursive partitioning using the rpart routines, 1997.
- [54] G. Van den Broeck, N. Di Mauro, and A. Vergari. Tractable probabilistic models: Representations, algorithms, learning, and applications. <http://web.cs.ucla.edu/~guyvdb/slides/TPMTutorialUAI19.pdf>, 2019. Tutorial at UAI 2019.
- [55] J. Vanschoren, J. N. van Rijn, B. Bischl, and L. Torgo. Openml: Networked science in machine learning. *SIGKDD Explorations*, 15(2):49–60, 2013.
- [56] V. N. Vapnik. *Statistical Learning Theory*. Wiley-Interscience, 1998.
- [57] K. Wu, K. Zhang, W. Fan, A. Edwards, and S. Y. Philip. Rs-forest: A rapid density estimator for streaming anomaly detection. In *2014 IEEE International Conference on Data Mining*, pages 600–609. IEEE, 2014.

A Theoretical Results

Proposition 1. *A GeDT is deterministic.*

Proof. Consider any sum node v in a GeDT and assume, for simplicity, that it has two children u' and u'' . Node v is associated with a partition $\{\mathcal{X}_{u'}, \mathcal{X}_{u''}\}$ of \mathcal{X}_v . Any leaf l which is a descendant of u' , respectively u'' , must have a support which is a subset of $\mathcal{X}_{u'}$, respectively $\mathcal{X}_{u''}$. Assume that $u'(x) > 0$ for certain x , implying $x \in \mathcal{X}_{u'}$ and thus $x \notin \mathcal{X}_{u''}$. Therefore, $u''(x) = 0$, since x is not in the support of any leaf below u'' . The same argument holds for the reverse case and straightforwardly extends to arbitrary many sum children. Thus v is deterministic. \square

Theorem 3. *Let f be a DT classifier and $p(Y | \mathbf{x})$ be a corresponding GeDT classifier, where each leaf in GeDT is class-factorised, i.e. of the form $p(Y)p(\mathbf{X})$, and where $p(Y)$ has been estimated in maximum-likelihood sense. Then $f(\mathbf{x}) = p(Y | \mathbf{x})$, provided that $p(\mathbf{x}) > 0$.*

Proof. Recall that the leaves in the GeDT are in one-to-one correspondence with the leaf cells \mathcal{A} of the DT, and that the support of any leaf is given by its corresponding $\mathcal{A} \in \mathcal{A}$. Let $v_{\mathbf{x}}$ be the unique leaf in the GeDT whose cell is $\mathcal{A}(\mathbf{x})$. Since GeDT is a tree-shaped PC containing only sum nodes, its joint distributions is either $p_{v_{\mathbf{x}}}(\mathbf{x}, y)$ —if GeDT consists only of $v_{\mathbf{x}}$ —or can be written as

$$p(\mathbf{x}, y) = \sum_{u \in \text{ch}(v)} w_{v,u} u(\mathbf{x}), \quad (2)$$

where v is the root node. Since the GeDT is deterministic, it has at most one non-zero child. From $p(\mathbf{x}) > 0$ it follows that the GeDT has *exactly* one non-zero child, say u' , and (2) can be written as $p(\mathbf{x}, y) = w_{v,u'} u'(\mathbf{x}, y)$. Now, since $u'(\mathbf{x}, y)$ is also a tree-shape PC containing only sums, it follows by induction that $p(\mathbf{x}, y) = \left(\prod_{(v,u) \in \Lambda} w_{v,u} \right) p_{v_{\mathbf{x}}}(\mathbf{x}, y)$, where Λ is the unique path from root to $v_{\mathbf{x}}$ following only non-zero nodes, and $w_{v,u}$ are the sum-weights of edges (v, u) in Λ . Since each leaf is class-factorised, we have $p_{v_{\mathbf{x}}}(\mathbf{x}, y) = p_{v_{\mathbf{x}}}(\mathbf{x}) p_{v_{\mathbf{x}}}(y)$, and $\left(\prod_{(v,u) \in \Lambda} w_{v,u} \right) p_{v_{\mathbf{x}}}(\mathbf{x}) p_{v_{\mathbf{x}}}(y) \propto p(y | \mathbf{x}) = p_{v_{\mathbf{x}}}(y) = f^{\mathcal{A}(\mathbf{x})}(\mathbf{x}) = f(\mathbf{x})$, since each $f^{\mathcal{A}(\mathbf{x})}$ is—like $p_{v_{\mathbf{x}}}$ —learned by the class proportions of samples falling in \mathcal{A} . \square

Theorem 4. *Let \mathbb{P}^* be an unknown data generating distribution with density $p^*(\mathbf{X}, Y)$, and let \mathcal{D}_n be a dataset drawn i.i.d. from \mathbb{P}^* . Let \mathcal{G} be a DT learned with a DT learning algorithm, using axis-aligned splits. Let \mathcal{A}^n be the (rectangular) leaf cells produced by the learning algorithm. Assume it holds that i) $\lim_{n \rightarrow \infty} |\mathcal{A}^n|^{\log(n)}/n \rightarrow 0$ and ii) $\mathbb{P}^*(\{\mathbf{x} | \text{diam}(\mathcal{A}_x^n) > \gamma\}) \rightarrow 0$ almost surely for all $\gamma > 0$, where $\text{diam}(\mathcal{A})$ is the diameter of cell \mathcal{A} . Let \mathcal{G}' be the GeDT corresponding to \mathcal{G} , obtained via Algorithm 1, where for each leaf v , p_v is of the form $p_v(Y)p_v(\mathbf{X})$, with $p_v(\mathbf{X})$ uniform on \mathcal{A}_v and $p_v(Y)$ the maximum likelihood Categorical (fractions of class values of samples in \mathcal{A}_v). Then the GeDT distribution is l_1 -consistent, i.e. $\sum_y \int |p(\mathbf{x}, y) - p^*(\mathbf{x}, y)| d\mathbf{x} \rightarrow 0$, almost surely.*

Before proving Theorem 4 we need to introduce some background. This theorem extends consistency results for collections of partitions of the state space \mathcal{X} , as discussed by Lugosi and Nobel [32]. A central notion is the *growth function* of such partitions.

Definition 1 (Growth function [32]). *Let \mathcal{X} be some set and \mathcal{F} be a collection of finite partitions of \mathcal{X} . Let $\xi = \{\xi_1, \dots, \xi_n\}$ be a set of points from \mathcal{X} . Let $\Delta(\mathcal{F}, \xi)$ be the number of distinct partitions induced by \mathcal{F} , that is the size of set $\{\{\xi \cap \mathcal{A} | \mathcal{A} \in \mathcal{A}\} | \mathcal{A} \in \mathcal{F}\}$. The growth function is defined as $\Delta^*(\mathcal{F}) = \sup_{\xi} \Delta(\mathcal{F}, \xi)$, where the sup ranges over all sets of n points in from \mathcal{X} .*

Note that the growth function Δ^* is defined akin to the *dichotomic growth function*, as introduced by Vapnik and Chervonenkis and well known in statistical learning theory [56]. In particular, we derive the following bound of Δ^* .

Proposition 2. *Let \mathcal{X} be some set and \mathcal{C} be any collection of subsets of \mathcal{X} . Let $\Phi(\mathcal{C}, \xi)$ be the shatter coefficient of point set ξ and $\Phi^*(\mathcal{C}) = \sup_{\xi} \Phi(\mathcal{C}, \xi)$ be the dichotomic growth function [56]. Let \mathcal{F} be a collection of finite partitions of \mathcal{X} , as in Definition 1, where the maximal partition size is $J := \sup_{\mathcal{A} \in \mathcal{F}} |\mathcal{A}|$. If $\mathcal{C} = \{\mathcal{A} | \mathcal{A} \in \mathcal{A}, \mathcal{A} \in \mathcal{F}\}$ then*

$$\Delta(\mathcal{F}, \xi) \leq \Phi(\mathcal{C}, \xi)^J, \quad (3)$$

and moreover $\Delta^(\mathcal{F}) \leq \Phi^*(\mathcal{C})^J$.*

Proof. Let the point set ξ be fixed. Any partition $\{\xi \cap \mathcal{A} \mid \mathcal{A} \in \mathcal{A}\}$, for some $\mathcal{A} \in \mathcal{F}$, can be written as $\{\xi \cap \mathcal{A}_1, \dots, \xi \cap \mathcal{A}_J\}$ for some $\mathcal{A}_1, \dots, \mathcal{A}_J \in \mathcal{C}$, since \mathcal{C} contains all cells which appear in \mathcal{F} . Thus, $\Delta(\mathcal{F}, \xi) \leq |\{\{\xi \cap \mathcal{A}_1, \dots, \xi \cap \mathcal{A}_J\} \mid \mathcal{A}_1, \dots, \mathcal{A}_J \in \mathcal{C}\}|$. Note that the number of partitions of this form is bounded by

$$|\{\{\xi \cap \mathcal{A}_1, \dots, \xi \cap \mathcal{A}_J\} \mid \mathcal{A}_1, \dots, \mathcal{A}_J \in \mathcal{C}\}| \leq \prod_{j=1}^J |\{\xi \cap \mathcal{A}_j \mid \mathcal{A}_j \in \mathcal{C}\}|. \quad (4)$$

The right hand side of (4) is $\Phi(\mathcal{C}, \xi)^J$, and thus (3) follows. $\Delta^*(\mathcal{F}) \leq \Phi^*(\mathcal{C})^J$ follows from applying \sup_{ξ} on both sides of (3). \square

In our case, we study partitions \mathcal{A} induced by a DT, each of which divides \mathcal{X} into a set of hyper-rectangles.⁴ Hence, we consider the collection of partitions \mathcal{F} containing all possible partitions whose sets are hyper-rectangles. We are not ready to prove Theorem 4.

Proof. Let \mathcal{F}^n be the collection of all DT partitions which can be generated for sample size n , i.e. $\mathcal{A}^n \in \mathcal{F}^n$. By Proposition 2, we know that $\Delta^*(\mathcal{F}^n) \leq \Phi^*(\mathcal{C})^{|\mathcal{A}^n|}$, where \mathcal{C} is the collection of all sub-rectangles in \mathcal{X} . The VC dimension [56] of \mathcal{C} is known to be $2|\mathbf{X}|$, and consequently, by Sauer's lemma, $\Delta^*(\mathcal{F}) \leq \Phi^*(\mathcal{C})^{|\mathcal{A}^n|} \leq Cn^{2|\mathcal{A}^n||\mathbf{X}|}$, where C is a constant depending only on $|\mathbf{X}|$. Therefore, if condition i) holds ($\lim_{n \rightarrow \infty} |\mathcal{A}^n|^{\log(n)/n} \rightarrow 0$) it follows that $\frac{\log \Delta^*}{n} \rightarrow 0$. Thus, together with condition ii) all conditions of Theorems 1 and 2 in [32] hold.

Since the GeDT is deterministic, its distribution can be written as

$$p(\mathbf{x}, y) = \left(\prod_{(v,u) \in \Lambda} w_{v,u} \right) p_{v_{\mathbf{x}}}(\mathbf{x}, y), \quad (5)$$

where $v_{\mathbf{x}}$ is the unique non-zero leaf in the GeDT, Λ is the unique path from the root to $v_{\mathbf{x}}$ following only non-zero nodes, and $w_{v,u}$ are the sum-weights of edges (v, u) in Λ (see also proof of Theorem 3).

It is easy to see that $\prod_{(v,u) \in \Lambda} w_{v,u} = \hat{\mathbb{P}}(\mathcal{A}_{\mathbf{x}})$, where $\hat{\mathbb{P}}$ is the empirical distribution of \mathcal{D}_n , i.e. the fraction of data points falling in $\mathcal{A}_{\mathbf{x}}$ (see Algorithm 1 in the main paper). The distribution computed by each leaf v is, by assumption, $p_v(\mathbf{x}, y) = p_v(y) \frac{1}{\text{vol}(\mathcal{A}_{\mathbf{x}})}$, where $\text{vol}(\mathcal{A})$ is the volume (Lebesgue measure) of \mathcal{A} . Thus, we can write (5) as

$$p(\mathbf{x}, y) = p_v(y) \hat{\mathbb{P}}(\mathcal{A}_{\mathbf{x}}) \frac{1}{\text{vol}(\mathcal{A}_{\mathbf{x}})}. \quad (6)$$

By Theorem 1 in [32], $\hat{\mathbb{P}}(\mathcal{A}_{\mathbf{x}}) \frac{1}{\text{vol}(\mathcal{A}_{\mathbf{x}})}$ converges to $p^*(\mathbf{x})$, while by Theorem 2 in [32], $p_v(y)$ converges to $p^*(y \mid \mathbf{x})$, both in $l1$ -sense. Clearly both factors, $\hat{\mathbb{P}}(\mathcal{A}_{\mathbf{x}}) \frac{1}{\text{vol}(\mathcal{A}_{\mathbf{x}})}$ and $p_v(y)$, have bounded $l1$ -norm. Thus, their product converges to $p^*(y \mid \mathbf{x}) p^*(\mathbf{x}) = p^*(y, \mathbf{x})$, which concludes the proof. \square

Corollary 3. *Under assumptions of Theorem 4, any GeDT predictor $p(Y \mid \mathbf{X}_o)$, for $\mathbf{X}_o \subseteq \mathbf{X}$ is Bayes consistent.*

Proof. Since $p(y, \mathbf{x})$ converges almost surely to $p^*(y, \mathbf{x})$ in $l1$ -sense, it gives rise to the Bayes optimal classifier $\arg \max_y p^*(y, \mathbf{x})$. Consider any $X_i \in \mathbf{X}$. The marginal distribution, X_i marginalised out, is $\int p(y, \mathbf{x}_{-i}, x_i) dx_i$. Since

$$\int |p(y, \mathbf{x}_{-i}) - p^*(y, \mathbf{x}_{-i})| dx_{-i} = \int \left| \int p(y, \mathbf{x}_{-i}, x_i) - p^*(y, \mathbf{x}_{-i}, x_i) dx_i \right| dx_{-i} \quad (7)$$

$$\leq \int |p(y, \mathbf{x}) - p^*(y, \mathbf{x})| dx, \quad (8)$$

also the marginal converges in $l1$ -sense to the true $p^*(y, \mathbf{x}_{-i})$. By repeating the argument, every sub-marginal converges, and thus gives rise to the corresponding Bayes optimal classifier. \square

⁴Here, we assume for simplicity that all variables are continuous. Including discrete variables with finitely many states can be done by applying similar arguments to each of the finitely many joint states.

Corollary 4. Assume a GeF whose GeDTs are learned under assumptions of Theorem 4. Then the GeF of GeDT predictors $p(Y | \mathbf{X}_o)$, for any $\mathbf{X}_o \subseteq \mathbf{X}$, is Bayes consistent.

Proof. This follows directly from Proposition 1 in [1], whereby if a sequence of classifiers is Bayes-consistent, then the classifier obtained by averaging them is also consistent. \square

B Time Complexity

Let n be the total number of samples and m the total number of features. Regarding the learning algorithm, a Random Forest and its corresponding PC only differ in the distributions at leaves, which use a partition of the data. Therefore, assuming a tree is grown as in [3] with $\lceil m/c \rceil$ features considered at each split (c a positive natural), structure learning in both models has worst-case asymptotic complexity of $\mathcal{O}(mr n \log n)$, where $r \in \mathcal{O}(n)$ is the number of internal nodes in the obtained tree [31]. For GeDTs, however, there is the additional cost of learning a distribution at each leaf. If $q(m)$ is the worst-case cost of the leaf learner for a constant amount of data, then the overall time complexity (for learning all leaves) is $\mathcal{O}(r q(m))$.

Nonetheless, if the leaf learner is such that $q(m) \leq \mathcal{O}(mn \log n)$, then the complexity is dominated by the structure learning and Random Forests and GeFs have the same worst-case asymptotic complexity of $\mathcal{O}(n_t (mr n \log n + r q(m))) \leq \mathcal{O}(n_t mr n \log n)$, where n_t is the number of trees in the model. Note that $q(m) \leq \mathcal{O}(mn \log n)$ holds for many learning algorithms when only a small number of training samples fall in each leaf—namely, LearnSPN and fully-factorised leaves—provided the reasonable assumption that m is $\mathcal{O}(n)$.

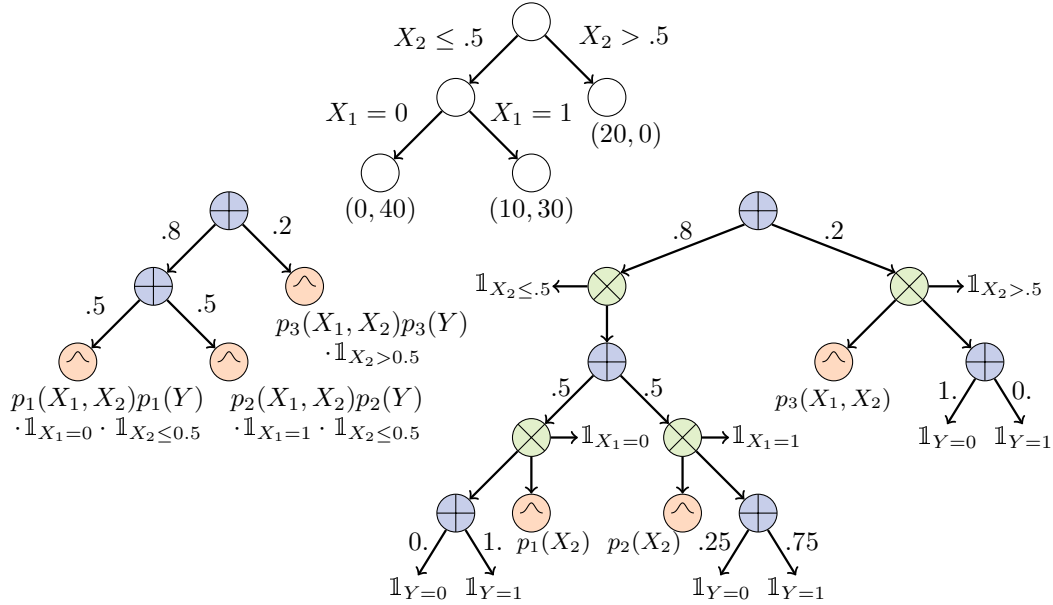


Figure 4: Illustration of pulling indicators up to speed up computations (in the example, \mathbf{X} and Y factorise at leaves). On top, the original decision tree (DT) is shown. Below, both models represent the probabilistic circuit for the original DT and encode the very same distribution, even if the one in the right-hand side is not decomposable.

On inference for a complete test sample, GeDTs require traversing the whole structure once (hence time $\mathcal{O}(r)$), while DTs have a worst-case of $\mathcal{O}(d)$, where d is the height of the tree. However, a clever idea brings the complexity of GeDTs down to $\mathcal{O}(d)$ by placing the indicators that define the decisions of the internal nodes of the DT near the corresponding internal nodes of the GeDTs. This requires augmenting GeDTs with product nodes, one for each internal sum node. Every new product node has two children: a sum node and an indicator mimicking the decision tree split, that is, it only evaluates to one if that path in the tree is active. Figure 4 illustrates the idea using the running

example of the main paper, where the densities are as follows

$$\begin{aligned} p_1(X_1, X_2, Y) &= p_1(X_1, X_2)(0 \cdot \mathbb{1}(Y = 0) + 1 \cdot \mathbb{1}(Y = 1)), \\ p_2(X_1, X_2, Y) &= p_2(X_1, X_2)(0.25 \cdot \mathbb{1}(Y = 0) + 0.75 \cdot \mathbb{1}(Y = 1)), \\ p_3(X_1, X_2, Y) &= p_3(X_1, X_2)(1 \cdot \mathbb{1}(Y = 0) + 0 \cdot \mathbb{1}(Y = 1)). \end{aligned}$$

Such idea does not change results, since it is just the very same as bringing the common indicators that appeared in the leaves of a sub-tree up towards the root of that sub-tree using the distributive property of multiplication (for the PC enthusiast, the lack of decomposability is tackled by the determinism of the indicators). By evaluating indicators as soon as possible in a top-down recursive computation, we can avoid computing all sub-trees for which a zero is returned to a product node [7]. With this type of computational graph, GeFs and RFs have a similar inference procedure. Predicting the class of an instance amounts to traversing each tree and evaluating the corresponding leaf, and thus the inference complexity is $\mathcal{O}(n_t d)$.

For incomplete data, however, GeDTs need to reach every active leaf (just as Friedman’s method). Assuming the number of missing values in each instance is bounded by a constant, GeFs still take time $\mathcal{O}(n_t d)$, while random forests with KNN imputation would take worst-case time $\mathcal{O}(n_t d + nm)$. In such case, GeFs are faster than random forests (RFs) with KNN imputation. For large (non-constant) percentages of missing values, GeFs can be as slow as $\mathcal{O}(n_t r)$ (as it may need to reach all leaves). In this case of great number of missing values per instance, GeFs are faster than RF with KNN imputation if $d \approx r$ but slower if $d \ll r$.

C Missing Values Experimental Results

All 21 datasets are listed here in alphabetical order. For each of them, we report (both in tabular and graphic formats) the accuracy values at different percentages of missing data at test time with 95% confidence intervals. These confidence intervals are computed across 10 repetitions of 5-fold cross validation for small datasets ($n < 10000$) and across a single 10-fold cross validation for larger ones. The datasets were obtained directly from the OpenML-CC18 benchmark web-page⁵ [55], and the only pre-processing step was standardising continuous features (mean $\mu = 0$ and standard deviation $\sigma = 1$) and mapping categorical features to $\{1, \dots, K_i\}$. The source code will be made available at the authors’ web-page.

We also present a few relevant details of each dataset.

- n: number of samples.
- m_0 : number of categorical variables.
- m_1 : number of numerical variables.
- $|\mathcal{Y}|$: number of classes.
- %Maj: percentage of the majority class.

For the sake of completeness, we briefly discuss each of the methods and their implementations. The source code is all in Python 3 and all experiments were run in a single laptop with a modern CPU.

Random Forest implementation In all experiments, the structure of all models is kept the same, that is, they are all derived from the same Random Forest and thus share the same partition of the feature space. For every dataset, the Random Forests were composed of 100 “deep” trees, that is, the only stop criterion is the impurity of the class variable, possibly leading to many leaves with a single sample. We used the Gini impurity measure as the criterion to select the best split in the decision-tree learning, and ranked surrogate splits according to how well they predict the best split, as in [53].

“Built-in” Methods These are methods for treating missing values that do not require external models, and hence are “built-in” into the decision tree structure. In fact, they consist of slight modifications to the inference procedure.

⁵<https://www.openml.org/s/99/data>

Surrogate splits [5, 53]: During training, once the best split is defined, one ranks alternative splits on the number of instances that they send to the same branch as the best split. At test time, if the split variable is not observed, one tries the surrogate splits in order (starting with that which most resembles the best split). If none of the surrogate split variables is available, the instance is sent to the branch with the highest number of data points at training time. Surrogate splits have two notable drawbacks: (i) their performance is heavily dependent on the correlation between variables; (ii) they require storing every possible split to be guaranteed to work for all missing-value configurations, which is rather computational intensive, especially for large ensembles.

Friedman method [15, 44]: Whenever a split variable is not observed, one follows both branches of the tree. That means any instance with missing value is mapped to multiple leaves, and the final prediction is given by the majority class across the sum of the counts of all these leaves. If $C^{\mathcal{A}}(j)$ gives the number of training instances of class j in cell \mathcal{A} , we can write Friedman’s methods as

$$f(\mathbf{x}) = \operatorname{argmax}_{j \in \{1, \dots, K\}} \sum_{\mathcal{A} \in \mathcal{A}} \mathbb{1}(\mathbf{x} \in \mathcal{A}) C^{\mathcal{A}}(j),$$

$$C^{\mathcal{A}}(j) = \sum_{i=1}^n \mathbb{1}(\mathbf{x}_i \in \mathcal{A}) \mathbb{1}(y_i = j),$$

where i runs through the n training instances (\mathbf{x}_i, y_i) , and j runs through the K possible classes.

Imputation methods It is not surprising that most of the work on handling missing data in decision trees and random forests rely on data imputation [50]. That is, another or multiple other models are used to predict the missing values before feeding the data to the tree-based classifier. In the experiments we compare two different types of imputation methods:

Mean: missing values are imputed with the mean for continuous variables or the most frequent observation for categorical variables.

KNN: similar to the simple method above but the means or most frequent values are taken over the K -nearest neighbours. We use a standard K -nearest neighbour implementation from scikit-learn [37] with $K=7$. However, the distance function is updated to better accommodate mixed data types. Following, Huang et al. [22], we define the distance measure as

$$d(\mathbf{x}_a, \mathbf{x}_b) = \gamma \sum_{i=0}^{m_0} w_i \delta(\mathbf{x}_a[i], \mathbf{x}_b[i]) + \sum_{i=m_0}^{m_1} \sqrt{w_i (\mathbf{x}_a[i] - \mathbf{x}_b[i])^2},$$

where γ is a parameter representing the relative importance of categorical and numerical features, w_i is the weight of feature i , and, without loss of generality, we assume features are ordered so that the first m_0 variables are categorical. The δ function is simply the Hamming distance: $\delta(\mathbf{x}_a[i], \mathbf{x}_b[i]) = 1$ if $\mathbf{x}_a[i] \neq \mathbf{x}_b[i]$, and $\delta(\mathbf{x}_a[i], \mathbf{x}_b[i]) = 0$ otherwise. As we have no reason to favour any feature or feature type, we set both γ and every w_i to one.

Vanilla GeFs What we call *vanilla* GeF, or simply GeF, is a model where the distribution at the leaves is given by a fully factorised model, that is, for each leaf v , $p_v(\mathbf{x}, y) = p_v(x_1)p_v(x_2) \dots p_v(x_m)p_v(y)$. This is probably the simplest model that one can fit at the leaves and is clearly *class-factorised*. Therefore, vanilla GeFs preserve full backward-compatibility with the original RF, yielding the exact same prediction function for complete data. We model the univariate distributions $p_v(x_i)$ as multinomial for categorical variables and normal for continuous ones.

LearnSPN models For GeF(LearnSPN) and GeF⁺(LearnSPN), the LearnSPN algorithm [17] is run only at leaves with more than 30 samples, and smaller leaves are modelled by a fully factorised model as in vanilla GeFs. That saves computational time with little performance impact, as the model derived from LearnSPN with few samples would be similarly simplistic. We run the LearnSPN algorithm as follows: sum nodes split the samples via K -means clustering with $K=2$, and product nodes split the variables with an independence threshold of 0.001 (pair of variables for which the

independence test yields a p-value lower than the threshold are considered independent). We do not force independence between the class Y and input variables X in LearnSPN, which explains why, in contrast to GeF, GeF(LearnSPN) does not necessarily yield the same predictions as the original Random Forest. LearnSPN eventually resolves in univariate distributions, and as for vanilla GeFs, we use multinomial and normal distributions for categorical and continuous variables, respectively.

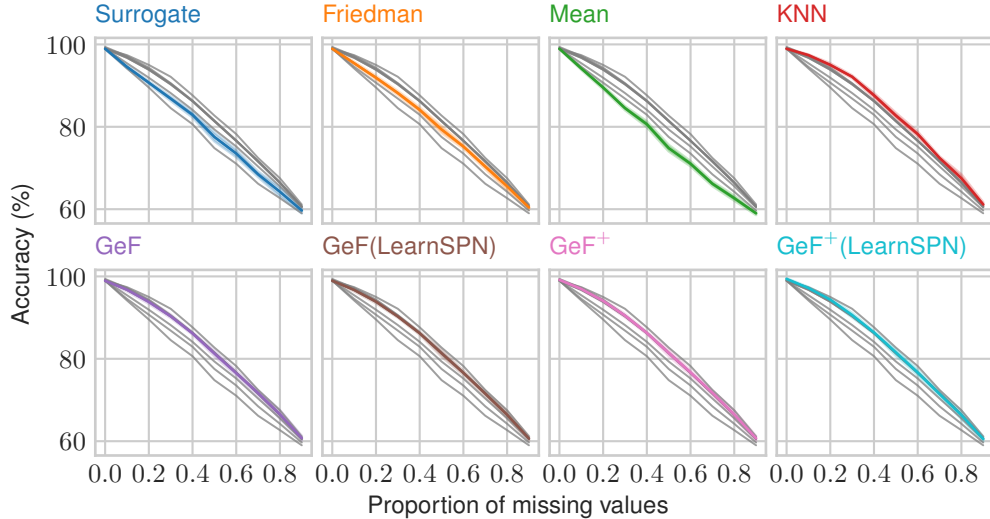
C.1 (Banknote) Authentication [12]

Dataset details

n	m ₀	m ₁	Y	%Maj
1372	0	4	2	55.54

Table 2: Accuracy per percent of missing values at test time.

(%)	Surr	Fried.	Mean	KNN	GeF	GeF(LSPN)	GeF ⁺	GeF ⁺ (LSPN)
0	98.95 ± .12	98.95 ± .12	98.95 ± .12	98.95 ± .12	98.95 ± .12	98.95 ± .12	99.16 ± .12	99.38 ± .15
10	94.55 ± .34	95.43 ± .33	94.16 ± .33	97.39 ± .15	96.77 ± .37	96.71 ± .33	96.95 ± .27	97.17 ± .26
20	90.7 ± .33	91.91 ± .42	89.53 ± .41	95.01 ± .39	93.81 ± .45	93.87 ± .38	94.07 ± .34	94.34 ± .38
30	86.84 ± .54	88.19 ± .47	84.53 ± .48	92.14 ± .31	90.33 ± .40	90.26 ± .27	90.47 ± .41	90.59 ± .55
40	82.92 ± .63	84.12 ± .57	80.63 ± .69	87.65 ± .53	86.17 ± .29	86.2 ± .35	86.28 ± .31	86.38 ± .32
50	77.54 ± 1.05	79.34 ± .81	74.83 ± .78	82.73 ± .66	81.3 ± .67	81.36 ± .82	81.44 ± .75	81.55 ± .79
60	73.51 ± .89	75.22 ± .47	71.03 ± .61	78.23 ± .58	76.52 ± .55	76.6 ± .50	76.68 ± .57	76.67 ± .65
70	68.46 ± .65	70.36 ± .58	66.18 ± .57	72.44 ± .36	71.69 ± .63	71.55 ± .63	71.75 ± .58	71.48 ± .61
80	64.23 ± 1.08	65.57 ± .94	62.67 ± .59	67.51 ± .95	66.52 ± 1.02	66.41 ± .90	66.49 ± .95	66.35 ± .96
90	59.67 ± .69	60.41 ± .54	59.0 ± .42	61.13 ± .53	60.73 ± .57	60.63 ± .53	60.69 ± .59	60.54 ± .61



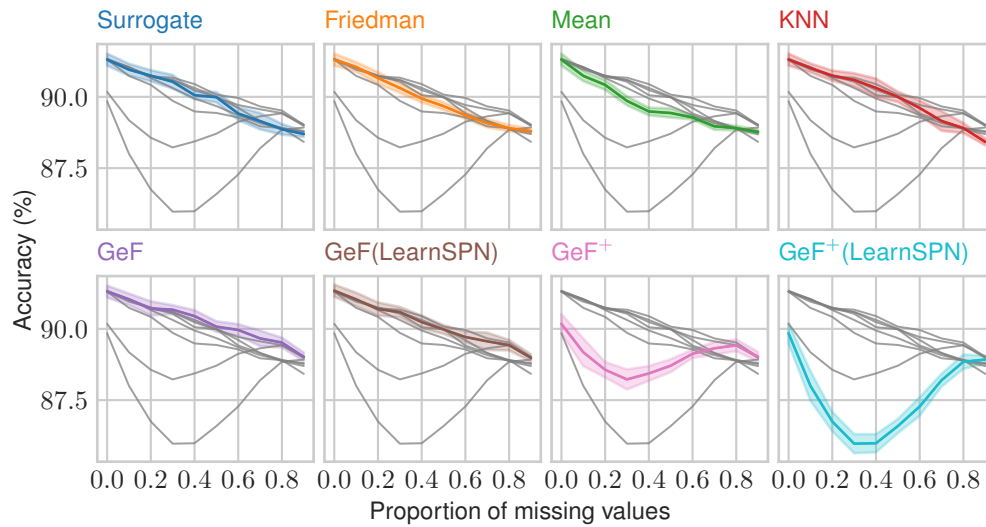
C.2 Bank Marketing [36]

Dataset details

n	m ₀	m ₁	\mathcal{Y}	%Maj
41188	11	9	2	88.73

Table 3: Accuracy per percent of missing values at test time.

(%)	Surr	Fried.	Mean	KNN	GeF	GeF(LSPN)	GeF ⁺	GeF ⁺ (LSPN)
0	91.31 ± .21	91.34 ± .21	90.17 ± .34	89.84 ± .36				
10	90.95 ± .21	91.05 ± .17	90.74 ± .19	91.01 ± .16	91.03 ± .20	91.03 ± .24	89.18 ± .49	88.0 ± .52
20	90.74 ± .20	90.66 ± .21	90.42 ± .17	90.74 ± .18	90.72 ± .25	90.69 ± .23	88.56 ± .27	86.75 ± .34
30	90.53 ± .24	90.31 ± .17	89.86 ± .16	90.59 ± .24	90.67 ± .16	90.59 ± .18	88.23 ± .35	85.97 ± .34
40	90.06 ± .15	89.94 ± .14	89.49 ± .13	90.31 ± .33	90.45 ± .21	90.24 ± .23	88.44 ± .26	85.99 ± .32
50	89.99 ± .18	89.67 ± .13	89.43 ± .16	90.0 ± .18	90.08 ± .19	89.98 ± .16	88.71 ± .23	86.59 ± .25
60	89.41 ± .23	89.35 ± .13	89.28 ± .07	89.61 ± .26	89.96 ± .20	89.71 ± .19	89.13 ± .14	87.28 ± .33
70	89.15 ± .29	89.08 ± .15	88.97 ± .13	89.15 ± .35	89.66 ± .27	89.56 ± .31	89.32 ± .22	88.2 ± .23
80	88.86 ± .19	88.9 ± .11	88.9 ± .08	88.9 ± .18	89.52 ± .17	89.43 ± .18	89.42 ± .21	88.85 ± .25
90	88.7 ± .11	88.8 ± .09	88.77 ± .09	88.42 ± .12	89.02 ± .16	88.98 ± .13	89.02 ± .17	88.92 ± .14



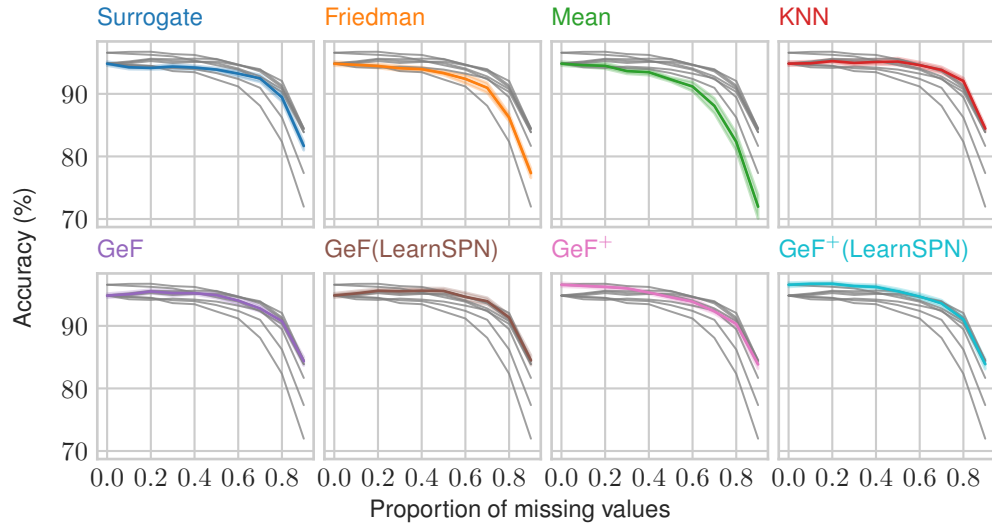
C.3 Breast Cancer (WDBC) ⁶

Dataset details

n	m ₀	m ₁	\mathcal{Y}	%Maj
569	0	30	2	62.74

Table 4: Accuracy per percent of missing values at test time.

(%)	Surr	Fried.	Mean	KNN	GeF	GeF(LSPN)	GeF ⁺	GeF ⁺ (LSPN)
0	94.83 ± .33	94.83 ± .33	94.83 ± .33	94.83 ± .33	94.83 ± .33	94.87 ± .35	96.57 ± .32	96.57 ± .35
10	94.25 ± .31	94.64 ± .28	94.59 ± .31	94.89 ± .35	95.06 ± .37	95.18 ± .41	96.4 ± .27	96.71 ± .30
20	94.15 ± .25	94.45 ± .33	94.48 ± .47	95.24 ± .28	95.5 ± .30	95.61 ± .32	96.24 ± .33	96.73 ± .30
30	94.36 ± .39	94.09 ± .39	93.64 ± .45	94.94 ± .47	95.24 ± .43	95.54 ± .47	95.99 ± .27	96.36 ± .33
40	94.2 ± .30	93.95 ± .32	93.46 ± .48	95.1 ± .41	95.22 ± .20	95.62 ± .44	95.33 ± .26	96.22 ± .35
50	93.88 ± .26	93.32 ± .32	92.3 ± .36	95.17 ± .56	94.92 ± .49	95.59 ± .45	94.59 ± .31	95.52 ± .42
60	93.23 ± .50	92.39 ± .73	91.18 ± .75	94.59 ± .50	94.04 ± .66	94.64 ± .68	93.87 ± .58	94.69 ± .46
70	92.48 ± .58	90.97 ± .80	88.08 ± 1.22	93.81 ± .50	92.78 ± .50	93.94 ± .56	92.32 ± .37	93.59 ± .53
80	89.46 ± .72	86.22 ± .62	82.34 ± 1.43	92.06 ± .49	90.76 ± .51	91.34 ± .47	90.32 ± .53	91.04 ± .55
90	81.67 ± .69	77.33 ± .77	71.97 ± 1.91	84.45 ± .47	84.32 ± .68	84.5 ± .81	83.85 ± .72	83.88 ± .82



⁶This breast cancer domain was obtained from the University Medical Centre, Institute of Oncology, Ljubljana, Yugoslavia. Thanks go to M. Zwitter and M. Soklic for providing the data.

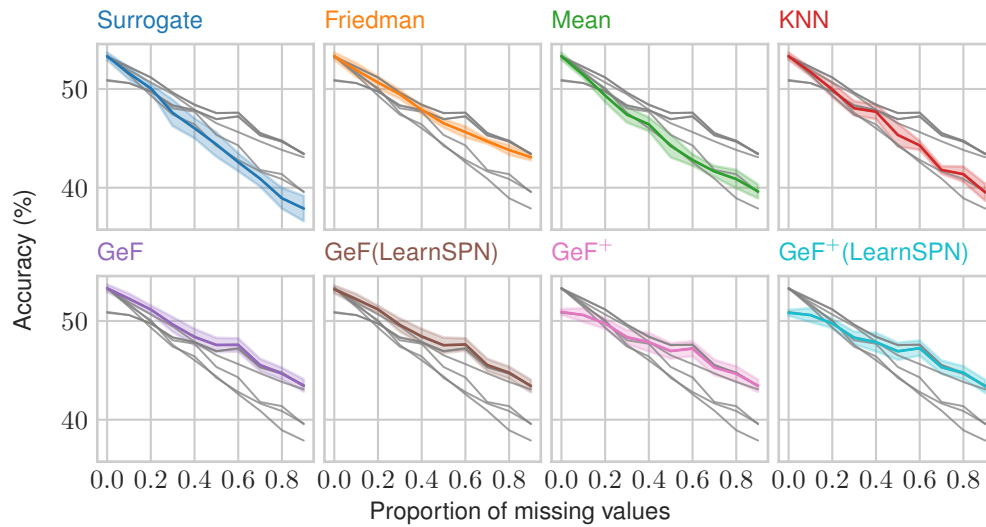
C.4 Contraceptive Method Choice (CMC) [12]

Dataset details

n	m ₀	m ₁	\mathcal{Y}	%Maj
1473	8	1	3	42.7

Table 5: Accuracy per percent of missing values at test time.

(%)	Surr	Fried.	Mean	KNN	GeF	GeF(LSPN)	GeF ⁺	GeF ⁺ (LSPN)
0	53.32 ± .37	53.2 ± .39	50.92 ± .29	50.83 ± .30				
10	51.58 ± .62	51.92 ± .71	51.43 ± .33	51.72 ± .42	52.27 ± .51	52.2 ± .55	50.6 ± .68	50.6 ± .71
20	50.07 ± .41	50.66 ± .60	49.33 ± .66	49.93 ± .74	51.15 ± .42	51.18 ± .36	49.74 ± .54	49.75 ± .48
30	47.58 ± 1.34	49.46 ± .46	47.4 ± .80	48.04 ± .73	49.65 ± .75	49.59 ± .66	48.36 ± .71	48.3 ± .63
40	46.02 ± 1.01	47.89 ± .43	46.42 ± .70	47.7 ± .75	48.37 ± .83	48.44 ± .76	47.85 ± .95	47.85 ± .95
50	44.39 ± 1.25	46.53 ± .43	44.24 ± 1.16	45.34 ± 1.18	47.58 ± .72	47.54 ± .78	46.97 ± .79	46.92 ± .87
60	42.59 ± .91	45.63 ± .56	42.81 ± .59	44.28 ± .45	47.58 ± .67	47.62 ± .63	47.19 ± .75	47.26 ± .77
70	40.92 ± .79	44.7 ± .24	41.65 ± .56	41.8 ± .39	45.54 ± .63	45.54 ± .63	45.29 ± .78	45.32 ± .68
80	38.93 ± 1.05	43.82 ± .49	40.88 ± .93	41.37 ± .77	44.66 ± .60	44.77 ± .61	44.65 ± .76	44.77 ± .65
90	37.89 ± 1.29	43.08 ± .31	39.62 ± .71	39.53 ± .88	43.47 ± .62	43.41 ± .63	43.43 ± .63	43.37 ± .67



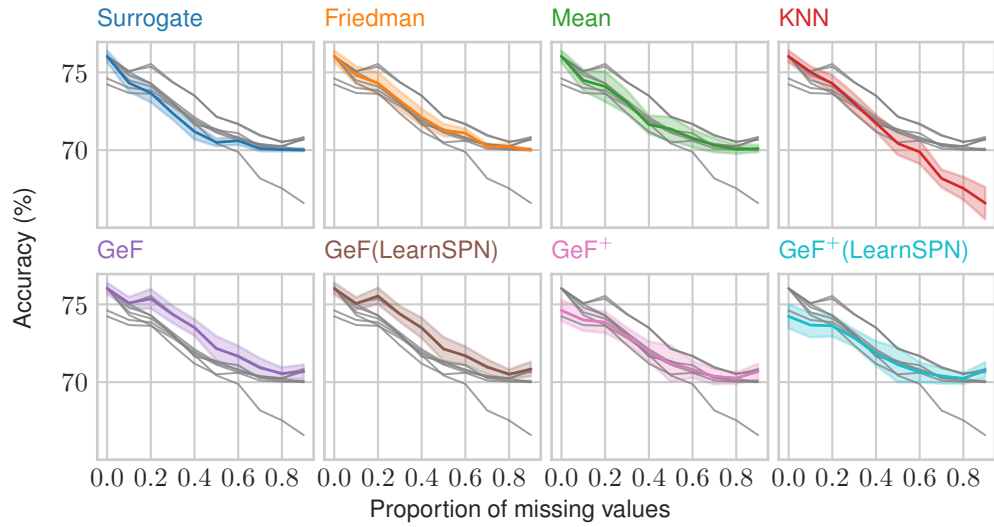
C.5 Credit-g [12]

Dataset details

n	m_0	m_1	$ \mathcal{Y} $	%Maj
1000	13	7	2	70.0

Table 6: Accuracy per percent of missing values at test time.

(%)	Surr	Fried.	Mean	KNN	GeF	GeF(LSPN)	GeF ⁺	GeF ⁺ (LSPN)
0	76.03 ± .38	76.02 ± .37	74.61 ± .68	74.23 ± .77				
10	74.32 ± .56	74.82 ± .58	74.49 ± .68	75.02 ± .38	75.09 ± .38	75.05 ± .41	74.0 ± .71	73.67 ± .79
20	73.67 ± .60	74.3 ± .72	74.09 ± .98	74.28 ± .54	75.36 ± .63	75.54 ± .53	73.85 ± .69	73.62 ± .69
30	72.37 ± .41	73.18 ± .60	73.09 ± .76	73.02 ± .60	74.35 ± .55	74.39 ± .51	72.97 ± .53	72.84 ± .55
40	71.19 ± .51	72.11 ± .57	71.64 ± .58	71.74 ± .54	73.51 ± .53	73.49 ± .65	71.97 ± .64	71.85 ± .78
50	70.5 ± .25	71.29 ± .40	71.36 ± .77	70.43 ± .74	72.17 ± .78	72.13 ± .76	71.19 ± 1.17	71.12 ± 1.12
60	70.6 ± .26	71.09 ± .29	70.76 ± .57	69.88 ± .76	71.65 ± .68	71.7 ± .59	70.82 ± .54	70.64 ± .64
70	70.1 ± .17	70.24 ± .16	70.31 ± .46	68.18 ± .58	70.92 ± .61	70.98 ± .49	70.36 ± .50	70.4 ± .50
80	70.03 ± .10	70.22 ± .17	70.06 ± .29	67.54 ± .74	70.56 ± .38	70.5 ± .31	70.26 ± .36	70.23 ± .35
90	70.0 ± .06	70.0 ± .06	70.1 ± .24	66.59 ± 1.04	70.67 ± .47	70.84 ± .47	70.68 ± .50	70.79 ± .49



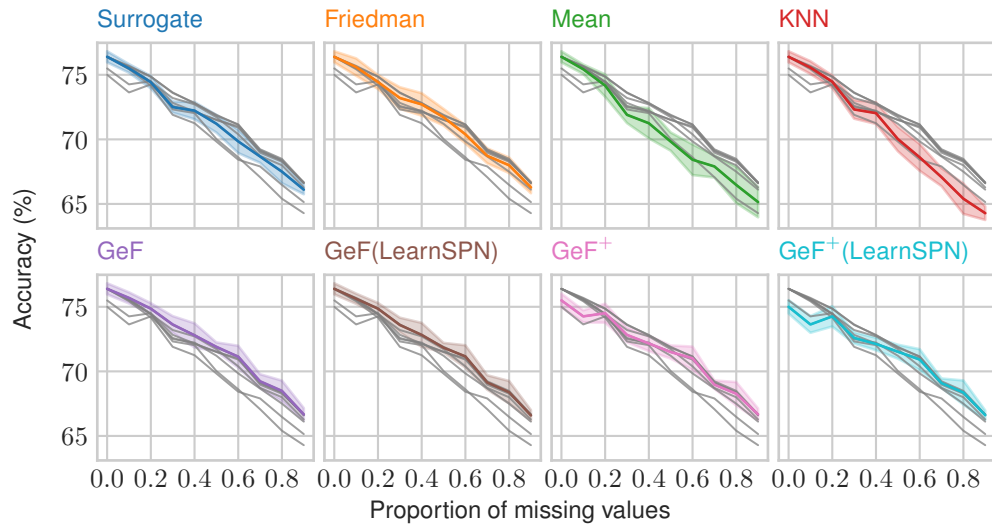
C.6 Diabetes [12]

Dataset details

n	m_0	m_1	$ \mathcal{Y} $	%Maj
768	0	8	2	65.1

Table 7: Accuracy per percent of missing values at test time.

(%)	Surr	Fried.	Mean	KNN	GeF	GeF(LSPN)	GeF ⁺	GeF ⁺ (LSPN)
0	76.39 ± .43	75.49 ± .53	75.0 ± .52					
10	75.49 ± .33	75.6 ± .67	75.43 ± .36	75.56 ± .49	75.69 ± .43	75.62 ± .39	74.26 ± .47	73.63 ± .65
20	74.43 ± .48	74.44 ± .54	74.17 ± .87	74.47 ± .48	74.86 ± .43	74.86 ± .44	74.51 ± .74	74.26 ± .79
30	72.5 ± .43	73.2 ± .84	71.9 ± .64	72.32 ± .72	73.63 ± .65	73.59 ± .56	72.83 ± .57	72.59 ± .44
40	72.23 ± .67	72.71 ± .87	71.25 ± 1.17	72.03 ± .83	72.79 ± .94	72.83 ± .93	72.16 ± .59	72.12 ± .48
50	71.21 ± .69	71.72 ± .64	69.83 ± .71	70.03 ± .94	71.9 ± .34	71.84 ± .37	71.5 ± .51	71.52 ± .54
60	69.84 ± .90	70.39 ± .70	68.42 ± 1.19	68.61 ± 1.04	71.13 ± .85	71.16 ± .86	71.02 ± .91	70.91 ± .81
70	68.67 ± .49	68.72 ± .58	67.9 ± .86	67.07 ± .70	69.23 ± .55	69.14 ± .56	68.97 ± .32	69.09 ± .36
80	67.5 ± .89	67.99 ± .60	66.47 ± 1.41	65.4 ± 1.18	68.49 ± .80	68.39 ± .87	68.27 ± .91	68.36 ± .94
90	66.11 ± .36	66.28 ± .45	65.14 ± 1.18	64.28 ± .53	66.67 ± .49	66.59 ± .41	66.67 ± .46	66.61 ± .36



C.7 DNA (Primate splice-junction gene sequences) [12]

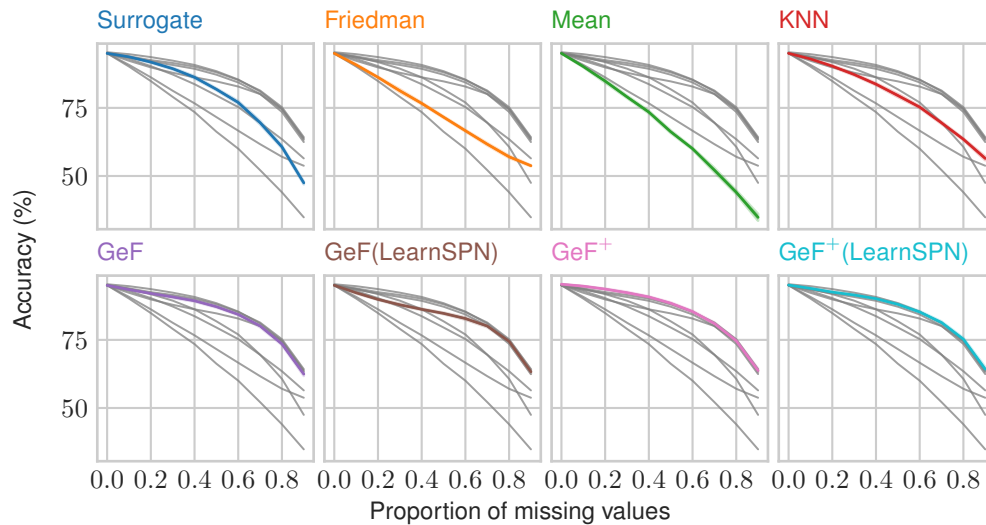
Dataset details

n	m ₀	m ₁	Y	%Maj
3186	180	0	3	51.91

This is the same dataset as Splice, but here the categorical variables were one-hot encoded.

Table 8: Accuracy per percent of missing values at test time.

(%)	Surr	Fried.	Mean	KNN	GeF	GeF(LSPN)	GeF ⁺	GeF ⁺ (LSPN)
0	95.02 ± .14	95.02 ± .14	95.02 ± .14	95.02 ± .14	95.02 ± .14	95.03 ± .15	95.42 ± .07	95.12 ± .14
10	93.72 ± .17	90.79 ± .32	90.17 ± .25	92.97 ± .21	93.46 ± .22	92.29 ± .30	94.71 ± .09	93.9 ± .23
20	91.8 ± .28	86.21 ± .22	84.83 ± .57	90.31 ± .31	92.04 ± .13	89.85 ± .16	93.64 ± .20	92.52 ± .18
30	89.4 ± .31	81.29 ± .56	79.04 ± .43	87.25 ± .36	90.75 ± .40	87.89 ± .42	92.33 ± .31	91.48 ± .28
40	86.23 ± .41	76.66 ± .32	73.45 ± .47	83.69 ± .35	89.34 ± .30	86.22 ± .23	90.76 ± .21	90.13 ± .25
50	81.82 ± .35	71.61 ± .31	66.25 ± .50	79.54 ± .55	87.18 ± .31	84.73 ± .29	88.47 ± .29	88.04 ± .39
60	76.98 ± .50	66.62 ± .32	60.02 ± .35	75.28 ± .38	84.33 ± .28	82.83 ± .42	85.4 ± .29	85.23 ± .33
70	69.59 ± .64	61.68 ± .44	52.15 ± .81	69.51 ± .42	80.12 ± .48	80.08 ± .44	81.0 ± .41	81.37 ± .39
80	60.69 ± .48	57.05 ± .42	44.02 ± .70	63.48 ± .32	73.51 ± .41	74.47 ± .39	74.67 ± .35	75.24 ± .47
90	47.47 ± .53	53.76 ± .22	34.81 ± 1.25	56.45 ± .67	62.44 ± .68	63.28 ± .80	63.74 ± .74	64.25 ± .79



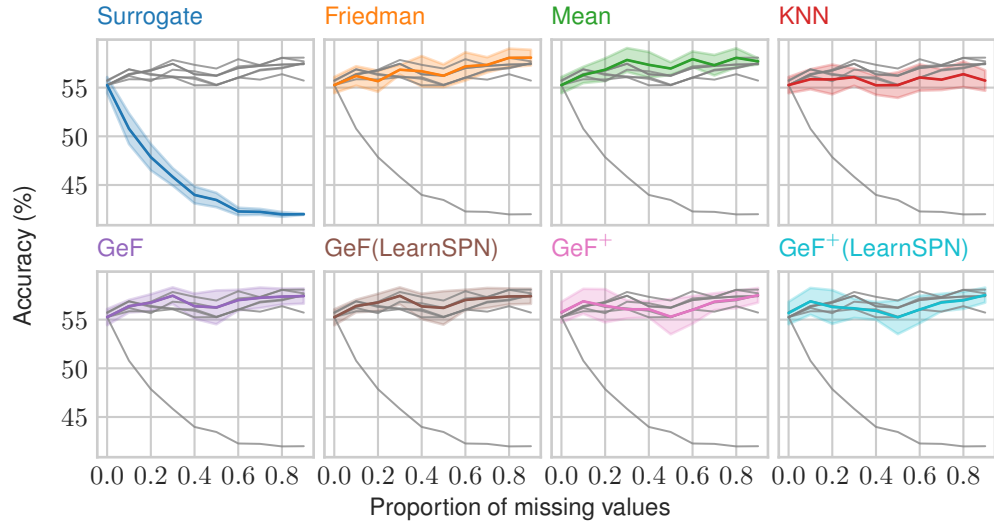
C.8 Dresses-sales [12]

Dataset details

n	m ₀	m ₁	\mathcal{Y}	%Maj
500	12	0	2	58.0

Table 9: Accuracy per percent of missing values at test time.

(%)	Surr	Fried.	Mean	KNN	GeF	GeF(LSPN)	GeF ⁺	GeF ⁺ (LSPN)
0	55.26 ± .83	55.26 ± .83	55.26 ± .83	55.26 ± .83	55.26 ± .83	55.24 ± .82	55.76 ± 1.07	55.68 ± 1.16
10	50.78 ± 1.58	56.2 ± 1.00	56.3 ± .83	55.86 ± 1.03	56.38 ± .64	56.4 ± .65	56.88 ± 1.28	56.88 ± 1.38
20	47.86 ± 1.36	55.66 ± 1.09	56.84 ± 1.16	55.84 ± 1.53	56.74 ± .87	56.76 ± .89	56.42 ± 1.71	56.3 ± 1.74
30	45.84 ± .90	56.84 ± .50	57.84 ± 1.23	56.08 ± .89	57.46 ± .86	57.44 ± .87	56.06 ± .93	56.16 ± .99
40	43.98 ± .87	56.68 ± 1.57	57.34 ± 1.32	55.24 ± .98	56.38 ± 1.30	56.36 ± 1.30	56.06 ± .84	55.9 ± .90
50	43.46 ± .74	56.22 ± 1.17	56.96 ± .65	55.26 ± 1.31	56.26 ± 1.74	56.2 ± 1.72	55.3 ± 1.81	55.24 ± 1.73
60	42.28 ± .38	57.18 ± 1.45	57.92 ± .80	56.04 ± 1.35	57.0 ± 1.06	57.02 ± 1.05	56.0 ± 1.43	56.04 ± 1.42
70	42.24 ± .31	57.34 ± .78	57.3 ± 1.05	55.82 ± 1.07	57.24 ± 1.06	57.22 ± 1.03	56.84 ± .87	56.76 ± .90
80	41.98 ± .24	58.06 ± .95	58.06 ± .98	56.38 ± 1.32	57.36 ± .82	57.38 ± .83	57.06 ± .88	56.98 ± .88
90	42.0 ± .06	58.08 ± .81	57.7 ± .32	55.72 ± 1.05	57.42 ± .78	57.4 ± .78	57.5 ± .76	57.52 ± .77



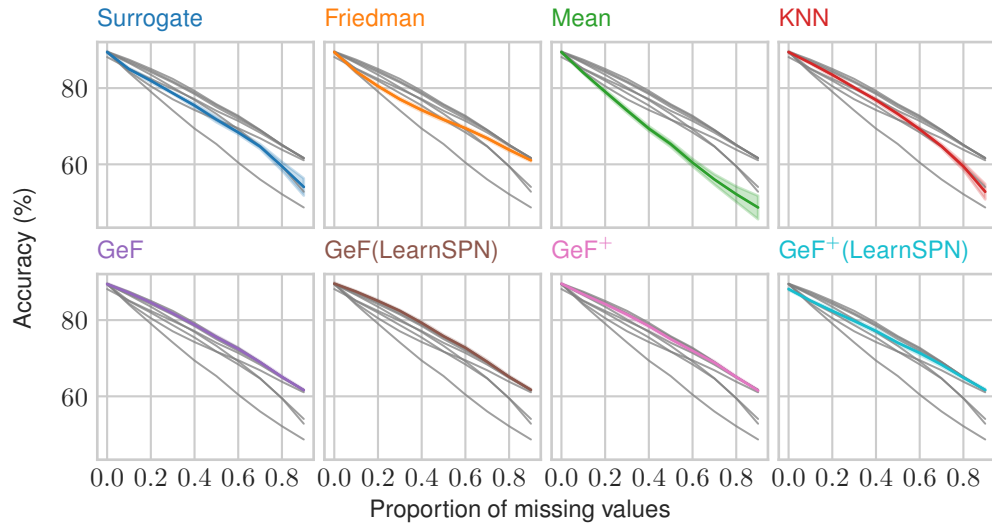
C.9 Electricity [16]

Dataset details

n	m_0	m_1	$ \mathcal{Y} $	%Maj
45312	1	7	2	57.55

Table 10: Accuracy per percent of missing values at test time.

(%)	Surr	Fried.	Mean	KNN	GeF	GeF(LSPN)	GeF ⁺	GeF ⁺ (LSPN)
0	89.45 ± .28	89.58 ± .28	89.54 ± .23	88.14 ± .26				
10	84.98 ± .33	84.36 ± .38	84.04 ± .24	86.57 ± .21	87.16 ± .25	87.46 ± .22	86.78 ± .29	85.11 ± .20
20	81.96 ± .43	80.5 ± .33	79.06 ± .56	83.51 ± .44	84.61 ± .31	85.03 ± .29	84.21 ± .29	82.4 ± .41
30	78.68 ± .22	77.08 ± .39	74.15 ± .62	80.17 ± .18	81.79 ± .31	82.43 ± .25	81.48 ± .51	79.8 ± .42
40	75.44 ± .49	74.24 ± .44	69.38 ± .64	76.89 ± .41	78.78 ± .32	79.26 ± .40	78.44 ± .36	77.12 ± .48
50	71.76 ± .70	71.72 ± .47	65.32 ± .75	73.24 ± .52	75.52 ± .46	75.78 ± .38	75.02 ± .43	74.04 ± .39
60	68.38 ± .50	69.47 ± .33	60.45 ± .97	69.17 ± .56	72.46 ± .36	72.74 ± .33	71.95 ± .45	71.39 ± .54
70	64.67 ± .64	66.84 ± .37	56.04 ± 1.36	64.74 ± .50	68.95 ± .33	69.05 ± .44	68.87 ± .40	68.32 ± .49
80	59.51 ± 1.16	63.83 ± .42	52.17 ± 2.05	59.47 ± .94	65.1 ± .34	65.12 ± .33	65.08 ± .28	64.9 ± .30
90	54.06 ± 2.27	61.06 ± .33	48.67 ± 3.08	52.81 ± 2.01	61.61 ± .24	61.7 ± .28	61.51 ± .31	61.67 ± .30



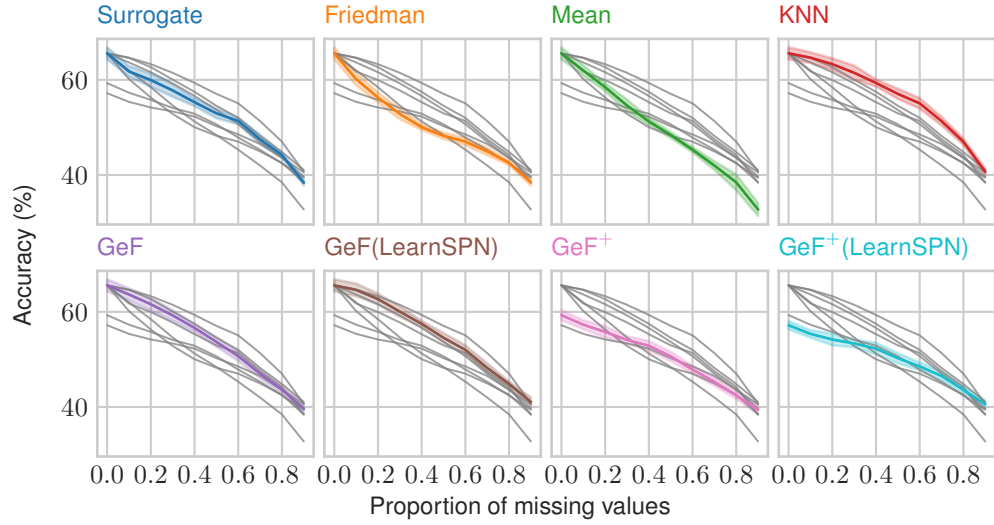
C.10 Gesture Phase Segmentation [33]

Dataset details

n	m_0	m_1	$ \mathcal{Y} $	%Maj
9873	0	32	5	29.88

Table 11: Accuracy per percent of missing values at test time.

(%)	Surr	Fried.	Mean	KNN	GeF	GeF(LSPN)	GeF ⁺	GeF ⁺ (LSPN)
0	65.57 ± 1.27	59.31 ± 1.07	57.2 ± .85					
10	61.76 ± 1.16	60.16 ± 1.32	61.98 ± 1.09	64.67 ± 1.14	63.66 ± 1.30	64.61 ± 1.35	57.3 ± .93	55.37 ± .79
20	59.95 ± 1.42	56.28 ± 1.06	58.45 ± .85	63.3 ± 1.22	61.6 ± 1.34	62.69 ± 1.14	55.79 ± 1.21	54.19 ± 1.24
30	57.77 ± 1.34	52.83 ± 1.16	54.61 ± 1.27	61.48 ± 1.52	59.25 ± 1.11	60.05 ± 1.13	54.1 ± .76	53.36 ± .82
40	55.3 ± .84	50.05 ± .58	51.25 ± .75	59.35 ± .74	56.62 ± .82	57.48 ± .64	52.88 ± 1.01	52.27 ± 1.25
50	52.96 ± 1.03	48.23 ± .70	48.41 ± .66	57.06 ± 1.08	53.69 ± 1.05	54.55 ± 1.01	50.65 ± .97	50.26 ± 1.08
60	51.36 ± .71	47.01 ± .78	45.32 ± .59	55.06 ± 1.11	50.68 ± 1.02	52.0 ± .97	47.87 ± .84	48.53 ± .84
70	47.5 ± .97	44.95 ± .82	41.98 ± .92	51.33 ± .91	47.0 ± .96	48.2 ± 1.01	45.3 ± .86	46.51 ± .97
80	44.2 ± .54	42.55 ± .50	38.44 ± 1.68	46.99 ± .68	43.62 ± .80	44.83 ± .53	42.43 ± .76	43.63 ± .76
90	38.37 ± .59	38.46 ± .75	32.74 ± 1.37	40.66 ± .78	39.66 ± 1.03	41.05 ± .99	39.42 ± 1.00	40.55 ± .91



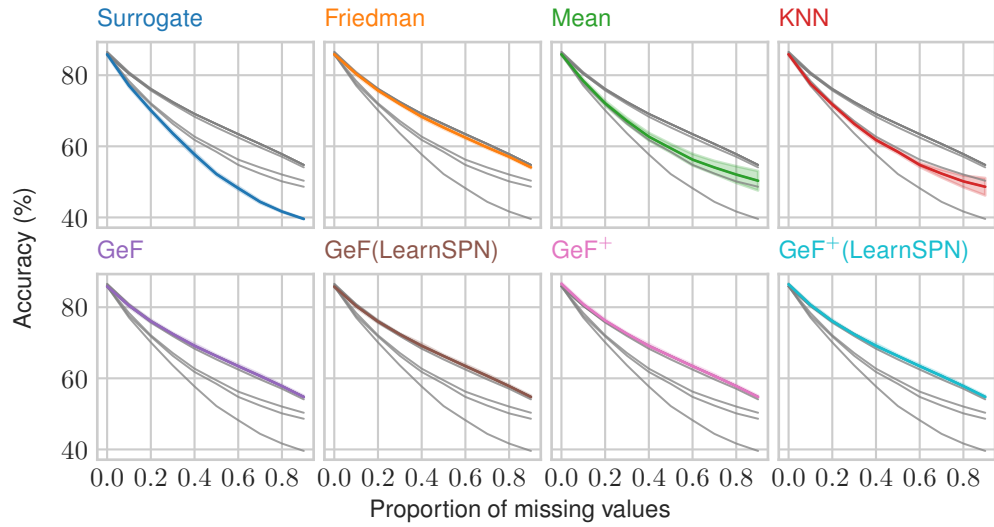
C.11 Jungle Chess [55]

Dataset details

n	m ₀	m ₁	\mathcal{Y}	%Maj
44819	6	0	3	51.46

Table 12: Accuracy per percent of missing values at test time.

(%)	Surr	Fried.	Mean	KNN	GeF	GeF(LSPN)	GeF ⁺	GeF ⁺ (LSPN)
0	85.88 ± .33	85.88 ± .33	85.88 ± .33	85.88 ± .33	85.88 ± .33	85.79 ± .30	86.6 ± .34	86.44 ± .27
10	77.08 ± .44	80.41 ± .49	78.39 ± .46	77.62 ± .45	80.45 ± .46	80.34 ± .44	80.84 ± .44	80.66 ± .43
20	70.12 ± .43	75.72 ± .37	72.1 ± .70	71.78 ± .45	76.07 ± .45	75.96 ± .40	76.24 ± .41	76.1 ± .41
30	63.65 ± .52	71.9 ± .27	67.12 ± .83	66.35 ± .48	72.5 ± .31	72.36 ± .27	72.53 ± .29	72.38 ± .26
40	57.71 ± .61	68.33 ± .45	62.72 ± 1.07	61.8 ± .51	69.14 ± .60	69.15 ± .64	69.11 ± .62	69.13 ± .63
50	52.21 ± .44	65.31 ± .41	59.46 ± 1.24	58.46 ± .46	66.26 ± .37	66.27 ± .35	66.26 ± .38	66.28 ± .36
60	48.22 ± .48	62.46 ± .36	56.26 ± 1.64	54.78 ± .58	63.42 ± .50	63.45 ± .47	63.42 ± .50	63.42 ± .47
70	44.39 ± .37	59.69 ± .35	54.05 ± 1.85	52.33 ± 1.11	60.68 ± .51	60.67 ± .49	60.66 ± .51	60.67 ± .49
80	41.66 ± .19	57.07 ± .31	52.06 ± 2.35	50.14 ± 1.65	57.81 ± .37	57.81 ± .37	57.81 ± .37	57.8 ± .37
90	39.58 ± .09	54.08 ± .30	50.32 ± 2.75	48.63 ± 2.45	54.77 ± .36	54.76 ± .37	54.77 ± .36	54.76 ± .37



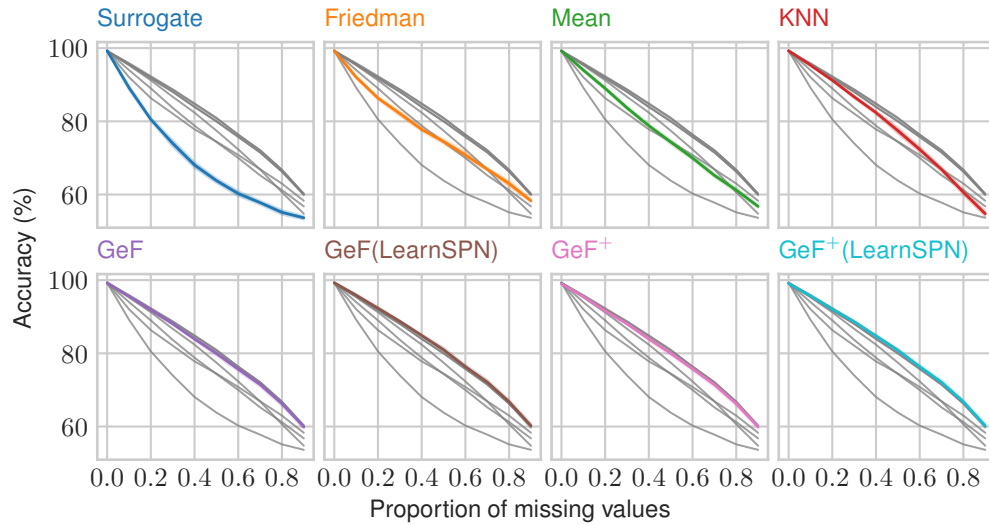
C.12 King-Rook vs. King-Pawn (kr-vs-kp) [12]

Dataset details

n	m ₀	m ₁	\mathcal{Y}	%Maj
3196	36	0	2	52.22

Table 13: Accuracy per percent of missing values at test time.

(%)	Surr	Fried.	Mean	KNN	GeF	GeF(LSPN)	GeF ⁺	GeF ⁺ (LSPN)
0	99.28 ± .05	99.28 ± .06	98.99 ± .09	99.09 ± .09				
10	89.2 ± .49	92.07 ± .30	94.0 ± .28	95.33 ± .15	95.56 ± .28	95.89 ± .22	95.53 ± .22	95.72 ± .23
20	80.52 ± .38	86.34 ± .32	89.01 ± .26	91.21 ± .12	91.89 ± .34	92.33 ± .29	91.61 ± .38	92.07 ± .27
30	73.98 ± .79	82.12 ± .54	83.69 ± .35	86.7 ± .30	88.06 ± .17	88.75 ± .15	88.07 ± .14	88.63 ± .23
40	68.07 ± .70	77.8 ± .43	78.8 ± .27	82.38 ± .33	83.93 ± .28	84.9 ± .19	83.95 ± .38	84.7 ± .31
50	63.81 ± .57	74.48 ± .52	74.36 ± .46	77.45 ± .67	79.97 ± .52	80.99 ± .47	80.03 ± .46	80.79 ± .43
60	60.26 ± .60	70.8 ± .67	69.99 ± .39	72.33 ± .61	75.69 ± .45	76.35 ± .42	75.83 ± .41	76.37 ± .40
70	57.79 ± .46	66.91 ± .32	65.24 ± .36	66.87 ± .51	71.51 ± .52	72.13 ± .56	71.48 ± .55	72.07 ± .57
80	55.13 ± .55	62.98 ± .73	61.22 ± .46	60.62 ± .57	66.25 ± .49	66.76 ± .42	66.25 ± .51	66.76 ± .42
90	53.64 ± .39	58.29 ± .36	56.76 ± .28	54.75 ± .63	59.91 ± .44	60.2 ± .55	59.93 ± .44	60.21 ± .55



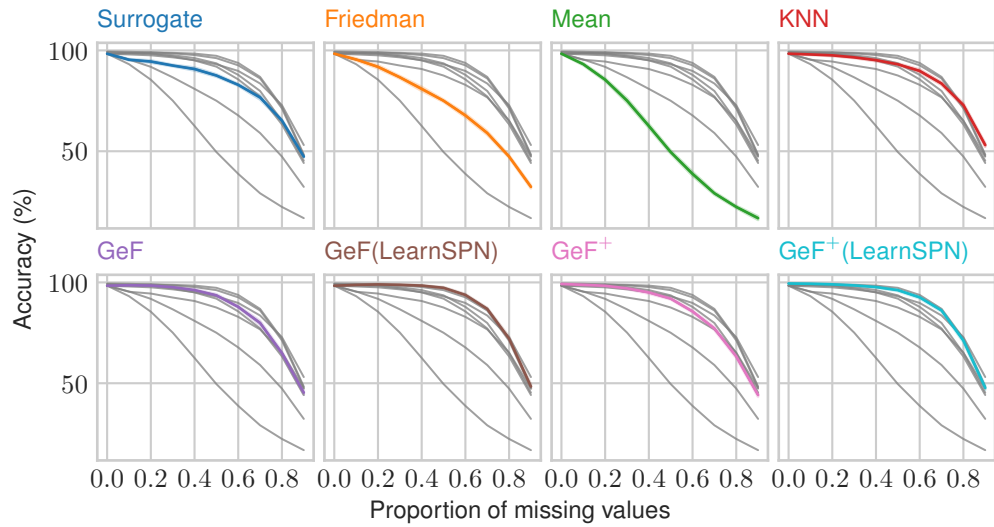
C.13 Mice Protein [21]

Dataset details

n	m ₀	m ₁	\mathcal{Y}	%Maj
1080	0	77	8	13.89

Table 14: Accuracy per percent of missing values at test time.

(%)	Surr	Fried.	Mean	KNN	GeF	GeF(LSPN)	GeF ⁺	GeF ⁺ (LSPN)
0	98.38 ± .16	98.38 ± .16	98.38 ± .16	98.38 ± .16	98.38 ± .16	98.36 ± .17	99.21 ± .17	99.45 ± .13
10	95.37 ± .32	95.49 ± .54	93.17 ± .53	97.99 ± .26	98.58 ± .25	98.77 ± .26	98.8 ± .33	99.31 ± .17
20	94.48 ± .56	91.84 ± .72	85.47 ± .67	97.56 ± .38	98.44 ± .19	99.0 ± .20	98.32 ± .32	99.02 ± .19
30	92.5 ± .40	86.66 ± .63	75.12 ± 1.04	96.56 ± .35	97.63 ± .26	98.79 ± .16	97.05 ± .43	98.51 ± .22
40	90.77 ± .74	80.92 ± 1.00	62.54 ± .96	95.17 ± .53	96.19 ± .37	98.42 ± .12	95.02 ± .60	97.69 ± .31
50	87.55 ± .58	75.04 ± .57	49.6 ± .80	93.1 ± .43	93.58 ± .57	97.31 ± .33	91.94 ± .40	96.17 ± .46
60	82.91 ± .43	67.75 ± .86	38.78 ± .99	89.81 ± .66	87.86 ± .43	93.78 ± .41	85.6 ± .50	92.59 ± .53
70	76.69 ± 1.05	59.03 ± .88	29.15 ± .69	83.58 ± .64	79.88 ± .95	86.86 ± .48	77.17 ± .80	86.08 ± .57
80	65.2 ± .53	47.35 ± .59	22.38 ± .56	72.85 ± .87	64.94 ± .81	72.11 ± .96	63.3 ± .80	71.21 ± .89
90	47.32 ± .46	32.32 ± .74	16.81 ± .90	53.06 ± .85	45.31 ± 1.07	48.33 ± 1.10	44.14 ± .90	47.72 ± .96



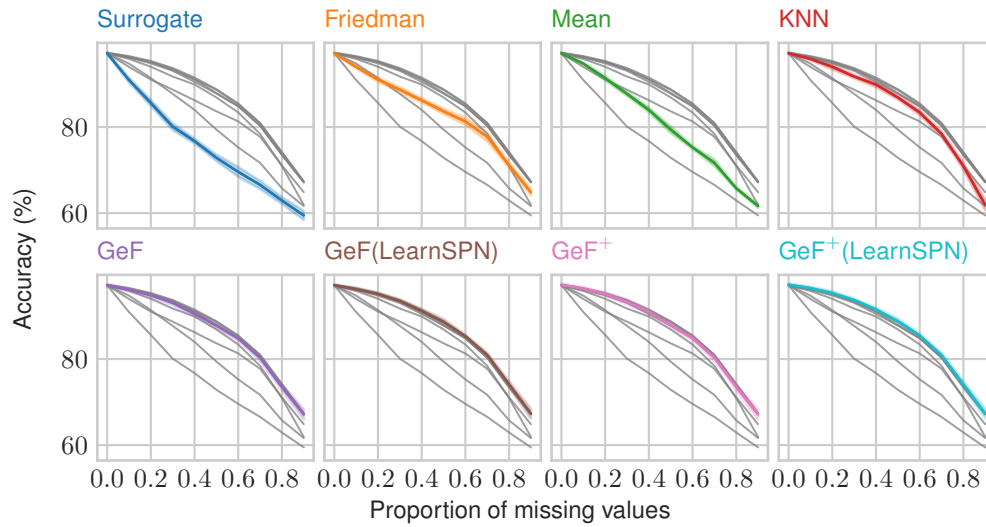
C.14 Phishing Websites [12]

Dataset details

n	m_0	m_1	$ \mathcal{Y} $	%Maj
11055	30	0	2	55.69

Table 15: Accuracy per percent of missing values at test time.

(%)	Surr	Fried.	Mean	KNN	GeF	GeF(LSPN)	GeF ⁺	GeF ⁺ (LSPN)
0	97.16 ± .25	97.14 ± .25	97.26 ± .31	97.3 ± .31				
10	90.94 ± .62	93.98 ± .35	94.75 ± .26	95.84 ± .33	96.14 ± .35	96.24 ± .33	96.37 ± .36	96.5 ± .36
20	85.61 ± .74	91.03 ± .55	91.37 ± .54	94.02 ± .61	94.82 ± .40	95.1 ± .39	95.15 ± .41	95.36 ± .42
30	80.1 ± .82	88.69 ± .63	87.72 ± .53	91.74 ± .44	93.07 ± .53	93.5 ± .42	93.31 ± .61	93.73 ± .37
40	76.73 ± .58	86.22 ± .55	83.99 ± .59	89.9 ± .64	90.51 ± .63	91.15 ± .53	91.03 ± .57	91.51 ± .46
50	72.86 ± .78	83.66 ± .64	79.41 ± .81	86.88 ± .51	87.79 ± .66	88.63 ± .70	87.89 ± .63	88.79 ± .63
60	69.58 ± 1.16	81.3 ± .85	75.27 ± .36	83.38 ± .61	84.79 ± .47	85.28 ± .40	84.88 ± .51	85.5 ± .44
70	66.55 ± .97	77.73 ± 1.11	71.67 ± .80	78.41 ± .56	80.3 ± .68	80.96 ± .54	80.32 ± .67	80.89 ± .58
80	62.92 ± .80	71.09 ± .69	65.75 ± .31	70.92 ± .84	73.49 ± .72	74.11 ± .77	73.55 ± .71	74.12 ± .79
90	59.46 ± 1.08	64.84 ± .83	61.63 ± .46	61.89 ± 1.23	67.13 ± 1.20	67.31 ± 1.16	67.15 ± 1.20	67.34 ± 1.15



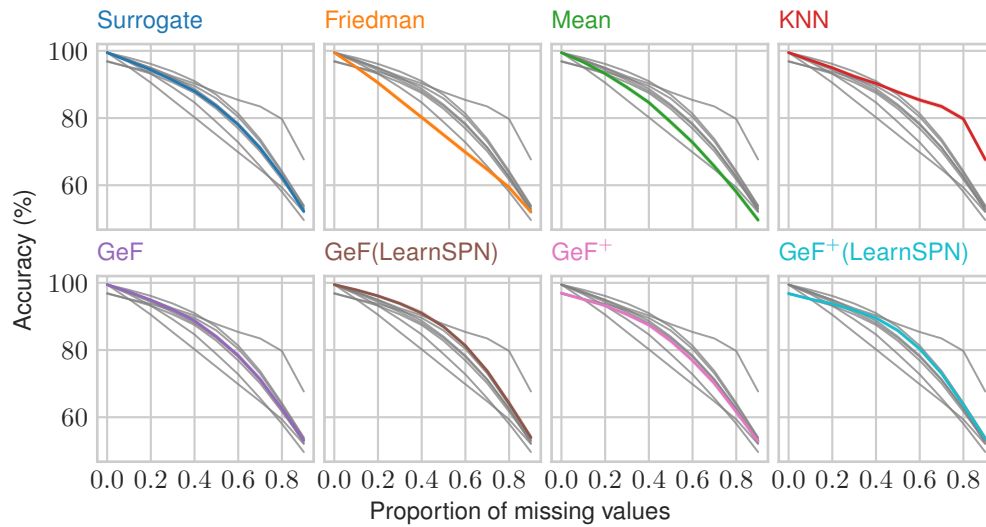
C.15 Robot (Wall-Following Robot Navigation) [12]

Dataset details

n	m ₀	m ₁	\mathcal{Y}	%Maj
5456	0	24	4	40.41

Table 16: Accuracy per percent of missing values at test time.

(%)	Surr	Fried.	Mean	KNN	GeF	GeF(LSPN)	GeF ⁺	GeF ⁺ (LSPN)
0	99.47 ± .03	96.94 ± .11	96.78 ± .11					
10	96.97 ± .15	95.14 ± .15	96.64 ± .19	97.21 ± .16	97.32 ± .17	97.91 ± .13	95.1 ± .17	95.16 ± .10
20	94.34 ± .10	90.5 ± .27	93.2 ± .19	94.95 ± .14	94.87 ± .18	96.1 ± .14	93.21 ± .15	93.75 ± .24
30	91.28 ± .29	85.32 ± .31	89.13 ± .33	92.41 ± .28	92.0 ± .31	93.85 ± .23	90.6 ± .21	91.84 ± .20
40	88.01 ± .25	80.2 ± .34	84.63 ± .28	90.3 ± .13	88.7 ± .30	90.98 ± .36	87.47 ± .26	89.55 ± .36
50	83.54 ± .28	75.01 ± .33	78.81 ± .34	87.71 ± .19	84.0 ± .22	86.95 ± .18	82.76 ± .37	85.82 ± .32
60	77.97 ± .23	69.82 ± .36	72.75 ± .32	85.38 ± .24	78.35 ± .26	81.29 ± .23	76.88 ± .18	80.34 ± .25
70	71.04 ± .55	64.71 ± .37	65.63 ± .38	83.45 ± .31	71.32 ± .47	73.74 ± .27	70.1 ± .39	73.03 ± .28
80	62.55 ± .26	59.33 ± .38	58.07 ± .42	79.72 ± .27	62.5 ± .45	64.19 ± .36	61.66 ± .43	63.62 ± .47
90	52.23 ± .24	52.05 ± .27	49.65 ± .37	67.67 ± .36	53.16 ± .38	53.98 ± .36	52.84 ± .42	53.66 ± .28



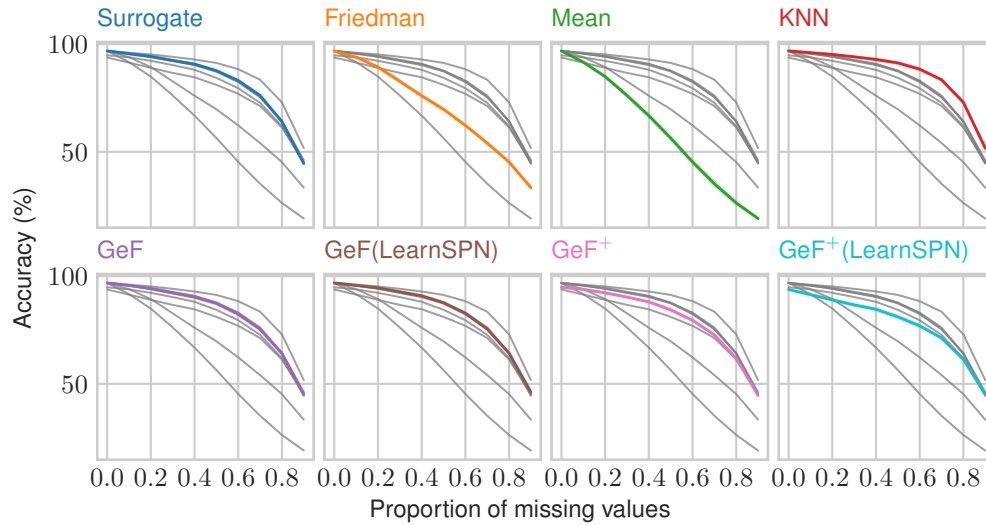
C.16 Segment [12]

Dataset details

n	m_0	m_1	$ \mathcal{Y} $	%Maj
2310	2	15	7	14.29

Table 17: Accuracy per percent of missing values at test time.

(%)	Surr	Fried.	Mean	KNN	GeF	GeF(LSPN)	GeF ⁺	GeF ⁺ (LSPN)
0	96.86 ± .17	96.87 ± .18	94.82 ± .25	93.8 ± .29				
10	95.52 ± .28	93.95 ± .35	91.67 ± .34	96.03 ± .22	95.72 ± .20	95.74 ± .24	93.87 ± .31	91.43 ± .38
20	94.23 ± .20	89.38 ± .44	84.95 ± .44	95.23 ± .13	94.13 ± .18	94.59 ± .18	92.25 ± .27	89.01 ± .53
30	92.39 ± .14	82.74 ± .34	76.17 ± .69	94.13 ± .18	92.18 ± .18	92.73 ± .20	90.29 ± .34	86.65 ± .47
40	90.71 ± .28	76.04 ± .55	66.8 ± .72	92.89 ± .42	90.23 ± .29	90.89 ± .37	88.09 ± .30	84.62 ± .45
50	87.65 ± .44	69.75 ± .46	56.4 ± .70	91.29 ± .35	87.34 ± .47	87.69 ± .38	84.36 ± .62	81.09 ± .61
60	83.11 ± .37	62.27 ± .28	45.31 ± .71	88.39 ± .44	82.33 ± .52	82.71 ± .41	79.52 ± .58	76.94 ± .73
70	76.16 ± .36	54.06 ± .35	35.17 ± 1.03	83.48 ± .39	75.34 ± .52	75.46 ± .60	72.73 ± .48	71.27 ± .41
80	64.03 ± .44	45.22 ± .35	26.25 ± .62	72.97 ± .42	64.1 ± .59	64.24 ± .42	61.87 ± .57	61.29 ± .51
90	44.56 ± .33	33.35 ± .31	19.01 ± .32	51.71 ± .68	45.14 ± .58	46.1 ± .72	44.64 ± .54	45.28 ± .70



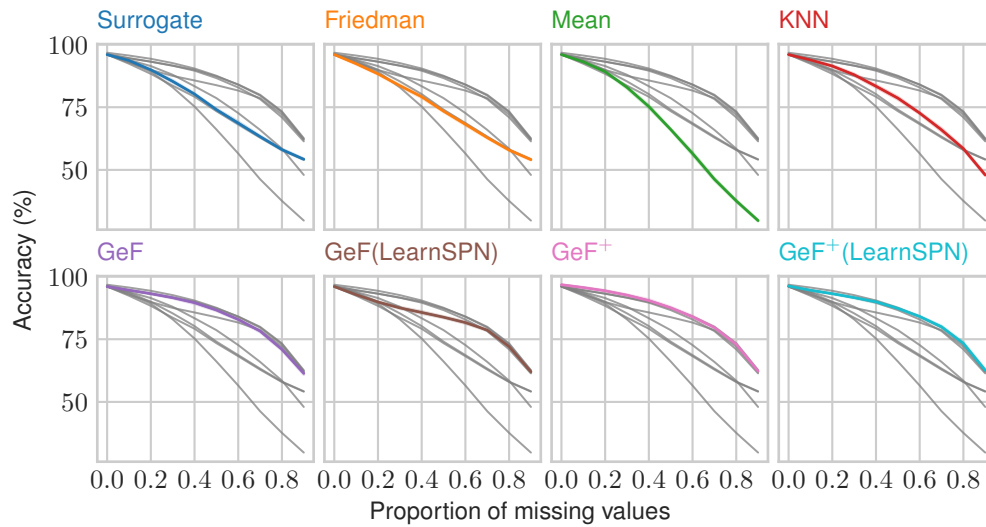
C.17 Splice (Primate splice-junction gene sequences) [12]

Dataset details

n	m ₀	m ₁	Y	%Maj
3190	60	0	3	51.88

Table 18: Accuracy per percent of missing values at test time.

(%)	Surr	Fried.	Mean	KNN	GeF	GeF(LSPN)	GeF ⁺	GeF ⁺ (LSPN)
0	96.0 ± .08	96.0 ± .08	96.0 ± .08	96.0 ± .08	96.0 ± .08	95.99 ± .09	96.73 ± .08	96.22 ± .15
10	93.63 ± .22	92.34 ± .25	93.12 ± .28	93.85 ± .20	94.56 ± .17	92.77 ± .21	95.61 ± .13	94.52 ± .17
20	89.91 ± .29	88.3 ± .24	89.17 ± .26	91.42 ± .33	93.16 ± .18	89.84 ± .25	94.31 ± .22	93.16 ± .15
30	85.31 ± .43	83.59 ± .36	82.92 ± .44	87.94 ± .38	91.55 ± .25	87.49 ± .34	92.59 ± .25	91.6 ± .26
40	80.23 ± .28	79.18 ± .43	75.27 ± .52	83.37 ± .48	89.57 ± .45	85.67 ± .46	90.43 ± .47	89.91 ± .44
50	74.04 ± .37	73.43 ± .30	66.13 ± .32	78.63 ± .52	86.62 ± .32	83.78 ± .31	87.55 ± .35	87.29 ± .28
60	68.67 ± .60	68.21 ± .45	56.54 ± .56	72.66 ± .34	82.87 ± .36	81.65 ± .41	83.97 ± .38	84.07 ± .21
70	63.29 ± .33	62.87 ± .27	46.29 ± .49	65.96 ± .60	78.24 ± .41	78.63 ± .28	79.66 ± .34	79.96 ± .38
80	58.1 ± .32	57.91 ± .29	37.64 ± .36	58.47 ± .36	70.96 ± .41	72.07 ± .35	72.98 ± .41	73.33 ± .50
90	54.24 ± .24	54.08 ± .26	29.79 ± .26	47.99 ± .38	61.38 ± .53	61.98 ± .44	62.26 ± .38	62.63 ± .48



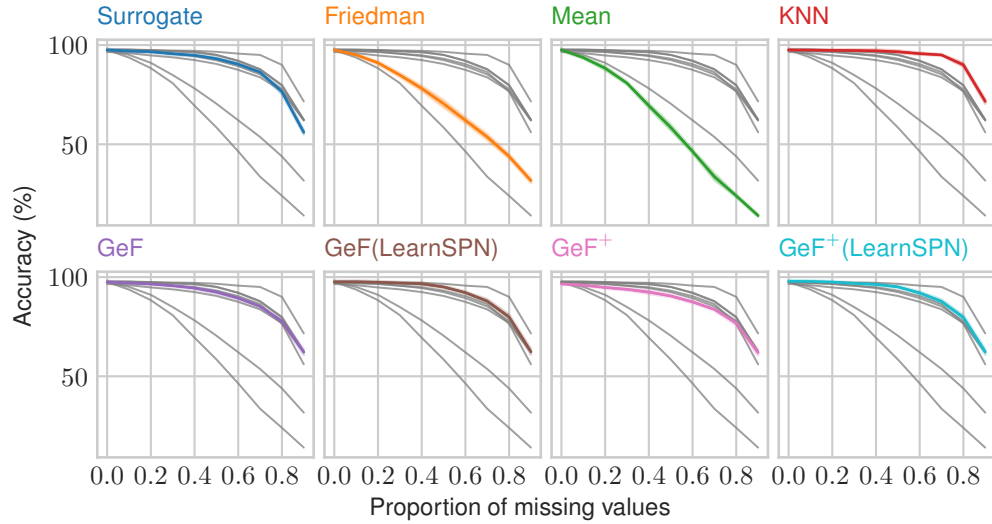
C.18 Texture ⁷

Dataset details

n	m ₀	m ₁	\mathcal{Y}	%Maj
5500	0	40	11	9.09

Table 19: Accuracy per percent of missing values at test time.

(%)	Surr	Fried.	Mean	KNN	GeF	GeF(LSPN)	GeF ⁺	GeF ⁺ (LSPN)
0	97.53 ± .54	97.53 ± .54	97.53 ± .54	97.53 ± .54	97.53 ± .54	97.55 ± .55	96.53 ± .29	97.89 ± .53
10	96.96 ± .59	95.05 ± .43	93.71 ± .61	97.45 ± .42	97.02 ± .60	97.6 ± .62	95.93 ± .44	97.78 ± .53
20	96.65 ± .49	91.05 ± .78	88.35 ± .93	97.31 ± .46	96.51 ± .39	97.4 ± .55	94.76 ± .51	97.49 ± .41
30	95.62 ± .62	84.89 ± 1.01	80.8 ± .75	97.25 ± .51	95.65 ± .47	97.0 ± .50	93.82 ± .60	96.8 ± .44
40	94.84 ± .52	78.16 ± 1.28	69.45 ± 1.19	97.09 ± .62	94.45 ± .58	96.67 ± .65	92.44 ± .93	96.31 ± .64
50	93.15 ± .81	70.47 ± 1.82	58.51 ± 1.49	96.62 ± .62	92.44 ± .82	95.02 ± .61	90.49 ± .61	95.07 ± .51
60	90.38 ± .70	62.09 ± 1.41	46.42 ± .95	95.69 ± .48	89.38 ± .69	92.18 ± .55	87.51 ± .66	91.95 ± .70
70	86.35 ± .61	53.69 ± 1.51	33.65 ± 1.62	95.02 ± .34	85.22 ± .83	87.89 ± .95	83.73 ± .59	87.67 ± 1.08
80	76.49 ± 1.28	43.89 ± 1.19	24.04 ± .75	90.02 ± .93	77.8 ± 1.12	79.89 ± 1.27	76.85 ± 1.17	79.6 ± 1.22
90	56.02 ± 1.05	31.69 ± 1.22	14.07 ± .67	71.62 ± 1.16	62.2 ± 1.43	62.38 ± 1.43	61.95 ± 1.53	62.29 ± 1.45



⁷This database was generated by the Laboratory of Image Processing and Pattern Recognition (INPG-LTIRF) in the development of the Esprit project ELENA No. 6891 and the Esprit working group ATHOS No. 6620.

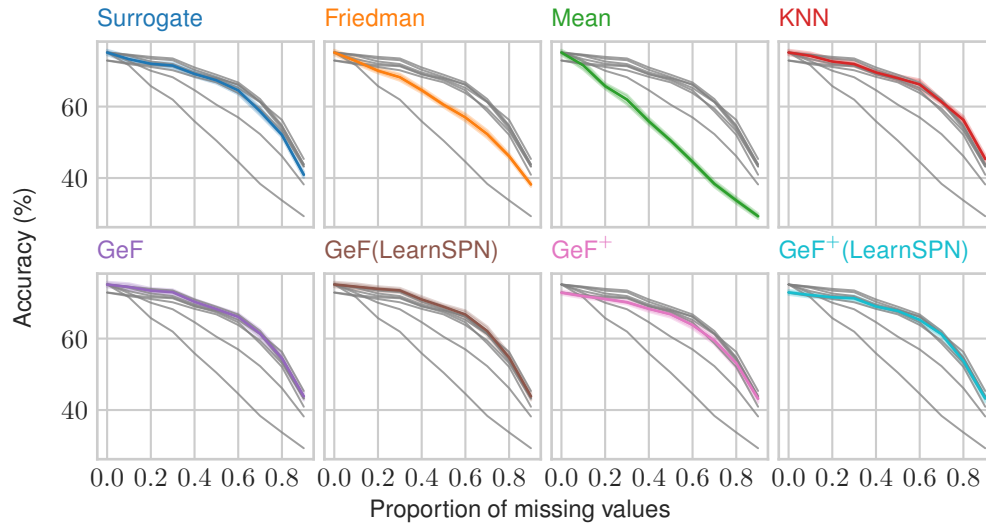
C.19 Vehicle [51]

Dataset details

n	m ₀	m ₁	\mathcal{Y}	%Maj
846	0	18	4	25.77

Table 20: Accuracy per percent of missing values at test time.

(%)	Surr	Fried.	Mean	KNN	GeF	GeF(LSPN)	GeF ⁺	GeF ⁺ (LSPN)
0	75.14 ± .68	75.14 ± .68	75.14 ± .68	75.14 ± .68	75.14 ± .68	75.14 ± .68	72.86 ± .52	72.92 ± .60
10	73.27 ± .83	72.72 ± .84	71.54 ± 1.16	74.2 ± .87	74.44 ± .95	74.54 ± .84	71.88 ± .56	72.17 ± .63
20	71.99 ± .44	70.04 ± .67	65.73 ± .74	72.62 ± .83	73.42 ± .66	73.91 ± .66	71.09 ± .51	71.56 ± .48
30	71.48 ± .76	68.22 ± .92	61.95 ± 1.29	71.9 ± .63	72.99 ± .70	73.48 ± .64	70.17 ± .54	71.29 ± .70
40	69.14 ± .84	64.59 ± .75	55.87 ± .94	69.55 ± .62	70.3 ± .72	70.95 ± .82	68.32 ± .79	68.98 ± .56
50	67.35 ± .86	60.52 ± .68	50.46 ± .79	67.96 ± .77	68.26 ± .69	68.91 ± .61	66.78 ± .86	67.74 ± .50
60	64.54 ± 1.07	56.96 ± 1.02	44.54 ± .87	66.21 ± 1.34	66.06 ± .91	66.74 ± 1.07	63.79 ± .97	65.22 ± 1.00
70	58.66 ± 1.04	52.28 ± 1.04	38.37 ± .85	61.34 ± .73	61.38 ± 1.11	62.1 ± 1.23	59.42 ± 1.00	61.23 ± .83
80	52.08 ± .64	46.12 ± .67	33.74 ± .84	56.26 ± 1.00	54.46 ± 1.22	54.72 ± 1.17	53.14 ± 1.42	53.76 ± 1.24
90	40.91 ± .81	38.19 ± .60	29.3 ± .71	45.33 ± 1.00	43.81 ± 1.06	43.81 ± 1.05	43.18 ± 1.11	43.26 ± 1.07



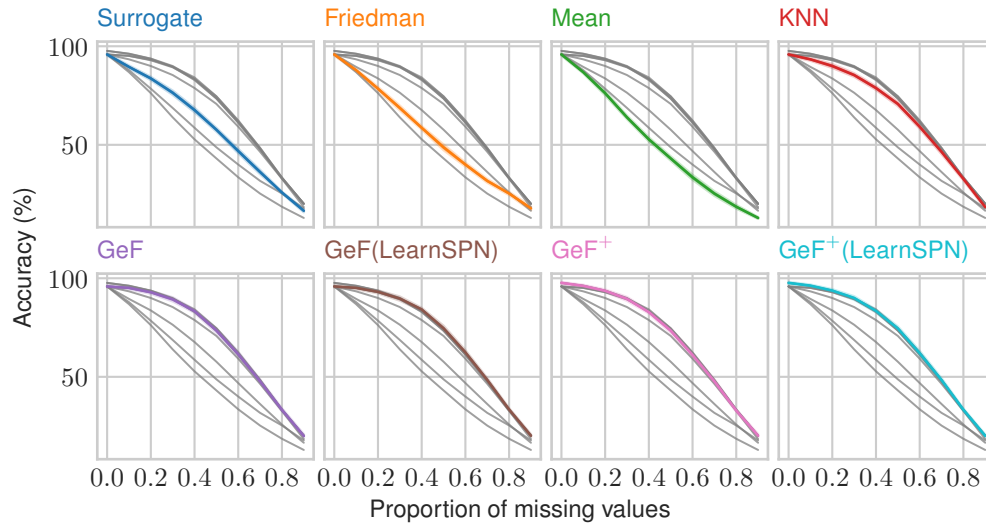
C.20 Vowel [12]

Dataset details

n	m ₀	m ₁	\mathcal{Y}	%Maj
990	2	10	11	9.09

Table 21: Accuracy per percent of missing values at test time.

(%)	Surr	Fried.	Mean	KNN	GeF	GeF(LSPN)	GeF ⁺	GeF ⁺ (LSPN)
0	95.85 ± .55	95.85 ± .55	95.85 ± .55	95.85 ± .55	95.85 ± .55	95.85 ± .55	97.68 ± .40	97.65 ± .44
10	89.53 ± .66	87.87 ± .52	86.85 ± .52	93.36 ± .63	95.11 ± .59	95.13 ± .62	96.13 ± .50	96.25 ± .49
20	83.68 ± .79	78.46 ± .86	76.21 ± 1.03	89.99 ± .90	92.89 ± .66	93.11 ± .70	93.63 ± .61	93.75 ± .64
30	76.42 ± 1.02	68.7 ± 1.10	63.93 ± .80	85.39 ± .85	89.3 ± .96	89.69 ± .99	89.55 ± .95	89.98 ± .85
40	67.65 ± 1.05	58.64 ± .81	52.79 ± .94	78.8 ± .86	83.33 ± .76	84.19 ± .73	82.83 ± .67	83.43 ± .67
50	57.67 ± .88	48.74 ± 1.38	43.1 ± .98	70.75 ± 1.02	73.54 ± 1.05	74.64 ± 1.22	73.45 ± 1.03	74.53 ± .98
60	46.84 ± 1.06	39.99 ± .93	33.53 ± 1.21	59.19 ± .96	61.48 ± 1.13	62.41 ± 1.03	61.08 ± 1.10	61.99 ± 1.13
70	36.2 ± 1.01	31.72 ± .86	25.27 ± 1.07	46.46 ± 1.10	47.72 ± .85	48.44 ± .82	47.7 ± .97	48.37 ± .87
80	25.81 ± .36	25.32 ± .77	18.59 ± .86	32.76 ± .68	33.25 ± .72	33.44 ± .59	32.9 ± .55	33.31 ± .54
90	16.56 ± .71	17.75 ± .89	12.91 ± .42	18.43 ± .63	20.01 ± .82	20.15 ± .66	20.15 ± .75	20.06 ± .63



C.21 Wine Quality [36]

Dataset details

n	m ₀	m ₁	\mathcal{Y}	%Maj
6497	0	11	2	80.34

This dataset includes both red and white wine data. For classification purposes, the target variable was split into two classes: scores less or equal to 6, and scores greater than 6.

Table 22: Accuracy per percent of missing values at test time.

(%)	Surr	Fried.	Mean	KNN	GeF	GeF(LSPN)	GeF ⁺	GeF ⁺ (LSPN)
0	88.89 ± .15	87.62 ± .15	86.21 ± .18					
10	86.52 ± .16	85.75 ± .15	86.41 ± .17	87.99 ± .18	88.1 ± .20	88.34 ± .19	87.54 ± .16	86.48 ± .26
20	85.14 ± .21	83.44 ± .13	84.36 ± .20	86.88 ± .19	86.88 ± .18	87.27 ± .16	87.1 ± .22	86.44 ± .26
30	84.0 ± .10	82.09 ± .07	82.73 ± .10	85.77 ± .14	85.52 ± .15	86.03 ± .14	85.94 ± .21	85.94 ± .14
40	82.8 ± .14	81.25 ± .06	81.73 ± .07	84.44 ± .15	84.17 ± .12	84.58 ± .14	84.76 ± .20	84.9 ± .22
50	81.99 ± .08	80.76 ± .09	81.14 ± .14	83.18 ± .18	82.84 ± .13	83.08 ± .11	83.31 ± .11	83.58 ± .11
60	81.4 ± .18	80.54 ± .06	80.72 ± .10	82.17 ± .11	81.85 ± .16	82.05 ± .14	82.21 ± .21	82.49 ± .21
70	80.91 ± .14	80.42 ± .03	80.45 ± .09	81.07 ± .20	81.21 ± .17	81.24 ± .15	81.4 ± .15	81.43 ± .17
80	80.57 ± .09	80.36 ± .02	80.35 ± .07	80.31 ± .21	80.68 ± .06	80.71 ± .06	80.72 ± .07	80.77 ± .07
90	80.43 ± .08	80.35 ± .01	80.36 ± .05	79.96 ± .18	80.46 ± .06	80.45 ± .05	80.46 ± .05	80.46 ± .04

